C.P. No. 1258

C.P. No. 1258

PROCUREMENT EXECUTIVE, MINISTRY OF DEFENCE

AERONAUTICAL RESEARCH COUNCIL

CURRENT PAPERS

The Nature, Development and Effect of the Viscous Flow around an Aerofoil with High - Lift Devices

by

D. N. Foster, P. R. Ashill and B. R. Williams

Aerodynamics Dept., R. A E, Farnborough

LONDON: HER MAJESTY'S STATIONERY OFFICE

1974

PRICE 80p NET

UDC 533.695.16 : 532.526 : 532.5.032

CP No.1258 *
December 1972

THE NATURE, DEVELOPMENT AND EFFECT OF THE VISCOUS FLOW AROUND AN AEROFOIL WITH HIGH-LIFT DEVICES

by

D. N. Foster
P. R. Ashill
B. R. Williams

Aerodynamics Dept., RAE, Farnborough

SUMMARY

This paper commences by describing the nature of the viscous flow around an aerofoil with high-lift devices, and considers a method of calculating the development of the viscous layers. The contributions of the wing wake and flap boundary layer to the lift carried by the components of the multiple aerofoil are then examined, and finally the manner in which the viscous layers may be incorporated into a calculation of the loading on the aerofoil is discussed.

---

* Replaces RAE Technical Report 72227 - ARC 34436

CONTENTS

1 INTRODUCTION

One of the long term aims of the work on high-lift wings is the achievement of the ability to predict the lift and pressure distribution around a high-lift aerofoil section given only the shape of the wing section and the Reynolds number, and also to design the shape of the aerofoil section for a given pressure distribution. This paper may be considered as a progress statement towards this goal.

As a background to the analytical discussions the general nature of the viscous flow around a wing section with mechanical high-lift devices is reviewed, noting especially those particular aspects of the flow where there are marked differences from the viscous flows normally experienced on wing sections without high-lift devices. The calculation of the development of these viscous flows is next considered, and the nature and accuracy of a calculation method recently developed at RAE is discussed.

In attempting to achieve the general analysis of the effects of the viscous layers it is essential to distinguish those elements of the viscous flow which have a marked influence on the flow around the wing section, and those whose influence is minimal. Whilst in the case of a single aerofoil the wake which lies downstream of the aerofoil might be expected not to have a decisive influence on the lift, with a slotted flap, the wake of the main aerofoil lies just above the flap, and thus may have a significant influence on the lift. The results of theoretical investigations into this effect, and on the problem of the extent to which details of the wake flow should be represented in the calculation, are discussed.

Finally the way in which those elements of the viscous flow, which have been found to have a profound influence on the flow, should be represented in a calculation of the flow around the wing is considered. The current approach to this problem is discussed, and the accuracy of the predictions resulting from this approach is illustrated. Indications are also given of an alternative approach giving the promise of improved accuracy.

2 GENERAL DESCRIPTION OF THE FLOW

The simplest high-lift configuration is, perhaps, the wing section without a leading-edge device, and with a slotted trailing-edge flap extended and deflected. The viscous flow around such a wing section is shown on Fig.1, together with a comparison of the pressure distribution measured on the wing

section with the flap deployed with that on the basic section without a high-lift device. The boundary layer which develops on the upper surface of the main wing is essentially similar to that which would develop on a simple wing section if it experienced the same pressure distribution. The viscous layer which develops on the lower surface of the wing shows one of a number of features which are peculiar to high-lift configurations, that is the separation and reattachment of the viscous layer just ahead of the trailing edge. The position of separation and the length of the separation bubble are dependent on the shape of the wing lower surface which exists when the flap has been deployed, but the presence of the bubble does not affect the mechanism of the stall.

However as the viscous layers from the upper and lower surfaces of the wing join at the wing trailing edge, and flow above the upper surface of the flap, the presence of the separation bubble on the lower surface of the wing does affect the second feature of the flow peculiar to high-lift configurations, the interaction between the wake from the wing and the boundary layer which develops on the upper surface of the flap. Experiments over a range of geometric positions of the flap relative to the wing have shown that when the flap is in the optimum position from the viewpoint of obtaining the highest maximum lift, the interaction between the wing wake and the flap boundary layer is comparatively mild, with the two layers retaining their separate identity almost to the flap trailing edge.

Two features of the pressure distributions are noteworthy. The presence of the flap has lowered the pressure coefficient at the trailing edge of the wing from its small positive value for the basic section to a negative value, which will increase in magnitude as the flap deflection increases. The second feature is the much increased severity of the adverse pressure gradient just downstream of the leading edge, so that there will be a tendency for the flapped wing section to exhibit a leading-edge stall, even if the basic section has a trailing-edge stall.

When a leading-edge device in the form of a slat is added to the wing section, the viscous flow becomes more complicated (Fig.2). The viscous layer which develops on the lower surface of the wing is similar to that described above for the wing section without a leading-edge device, and includes a separation bubble just ahead of the wing trailing edge. The boundary layer which develops on the upper surface of the wing is influenced by the presence of the wake from the slat just above the surface of the wing. It is found that,

for geometric positions of the slat which give optimum aerodynamic performance, there is a strong interaction between the slat wake and the wing boundary layer, so that close to the wing trailing edge the two layers tend to become merged. As described above, the viscous flow above the flap is characterised by weak interference between the combined wake from the wing and slat, and the boundary layer on the flap.

The pressure distributions also shown on this figure demonstrate the effect of the downstream elements of the multiple aerofoil on the pressure coefficients at the trailing edge of the upstream elements. The pressure distribution illustrated for the wing section without a leading-edge device (obtained by extrapolation beyond the stall to the angle of incidence (15^{o}) considered for this figure) emphasises the benefit of the slat in reducing the leading-edge suction peak, to be set against the adverse effect of the slat wake on the development of the boundary layer on the wing.

3 CALCULATION METHOD FOR WAKE-BOUNDARY LAYER INTERACTION

The method to be reported here is that developed by Irwin[1]. It is an integral method, in which the flow is assumed to consist of three regions (Fig.3):

(a) A boundary layer, whose velocity profile is assumed to be a power law;

(b) an inner wake region, whose velocity profile is assumed to be of Gaussian form; and

(c) an outer wake region, whose velocity profile is also assumed to be of Gaussian form.

A total of six variables are required to define the velocity profile of the complete viscous layer, and the numerical value of each of these six quantities varies in the streamwise direction. Integration of the momentum equation for the viscous layer in a direction normal to the stream over five different intervals will yield five of the six equations necessary for the evaluation of these six quantities; the sixth equation is an expression for the rate of change of mass flow in the region below the velocity minimum in the wake (the junction of the inner and outer wake regions). The solution of these six equations requires assumptions to be made regarding the shear stress at five positions in the viscous layer, and also regarding the mass flow across the line of minimum velocity. The particular assumptions made, and the effect of changes of these assumptions, are fully discussed by Irwin, and it is intended here only to

illustrate the results of the application of his method, using his 'best' assumptions.

Considering then specific comparisons between experimental values and the predictions of the calculation method, Fig.4 shows some velocity profiles measured above the flap when tested in conjunction with a plain leading edge. The calculations were commenced with the integral parameters for the three components of the viscous layer which were measured at the first station downstream of the trailing edge of the wing. It may be noted that the velocity profile of the inner wake is distinctly non-Gaussian - this form of the velocity profile has resulted from the separation bubble which existed on the lower surface of the wing, adding a viscous layer of small total head deficit to the inner edge of the wake. The presence of this non-Gaussian velocity profile does, in some cases, lead to discrepancies between the measured and predicted velocity profiles in the viscous layer. The calculations were made with the measured surface pressure distribution and the measured pressure gradient normal to the surface.

Comparisons between experiments and the calculation method can be made for a variety of quantities, and Irwin chose to make comparisons for each of the component layers of the total viscous layer. The comparisons presented here are for the displacement thickness of the total layer, a quantity which will be used later in the discussion of the calculation of the effect of the viscous flows on the circulation. Fig.5 shows that the prediction method is in quite reasonable agreement with the measured values upstream of the position at which the boundary layer separates from the flap: downstream of this point the calculations, although plausible numerically, cannot be expected to represent the real flow.

The velocity profiles measured in the viscous layer, when a slat is fitted, are shown on Fig.6. The marked difference between the interaction above the wing and that above the flap is clearly shown; it is hard to distinguish the part of the velocity profile at the wing trailing edge which can be ascribed to the presence of the slat, whereas the boundary layer on the flap at the flap trailing edge appears to be substantially unaffected by the combined wake from the wing and slat.

Irwin's method was specifically developed for the flow over a flap, where there is a pronounced minimum in the velocity profile. Fig.7 shows that it is also applicable to the flow above the wing, and does in general give as good agreement as for the flow above the flap, although the discrepancy for the

experimental value just ahead of the wing trailing edge might be attributed to the disappearance of the velocity minimum. For interest a curve has been added to Fig.7 of the displacement thickness which would be predicted by a calculation for a single boundary layer. It can be seen that the presence of the slat wake, and its effect on the development of the boundary layer on the wing, combine to increase the displacement thickness by a factor of just about 2, at the wing trailing edge, over the value predicted for a single boundary layer.

The final figure in the section cannot strictly be termed a comparison, since only two experimental points are available (Fig.8). It does, however, illustrate how the calculation method can be used to interpolate the extra values which will be required in the calculation of the effect of the viscous layers on the circulation.

In summary it can be said that the calculation method works reasonably well and for a rather wider range of configurations than might have been expected. It does not appear to be unduly sensitive to changes in the assumptions necessary, but will, of course, fail if the actual velocity profiles differ markedly from those assumed.

4 INFLUENCE OF WAKE OF MAIN AEROFOIL ON LIFT

4.1 Introductory remarks

It has previously been noted that viscous effects perform an important rôle in dictating the flow around multiple aerofoils. In particular, the existence of an optimum flap gap for lift at a given incidence can be associated with the presence of viscosity in the flow. The development of a model of the flow in which allowance can be made for viscous effects is therefore necessary if research on the characteristics of multiple aerofoils is to progress on other than purely empirical lines.

Fortunately, there is a significant amount of experimental data[2] available which will be invaluable in the search for an appropriate flow model. Some of these data for the velocity profiles in the viscous layers above the flap of an unslatted wing have already been shown on Fig.4. It is seen that, apart from the fact that the wake of the main aerofoil lies just above the flap, the aerofoil wake is quite thick when referred to the flap chord. Consequently, conventional methods of allowing for viscous effects[3,4] which are based on the notion that the viscous layers are 'thin', may be inappropriate for dealing with this type of flow. In this section, therefore, an attempt is made to answer the

following two questions. First, how large is the effect of the aerofoil wake on lift in comparison with that due to the flap boundary layer? Second, in instances when the wake effect is important, is the conventional approximation for 'thin' wakes adequate as a means of representation?

This section deals solely with a configuration which comprises an aerofoil having a drooped nose and a plain, Fowler flap set at an angle β of 30°. Only one angle of incidence, $\alpha = 0^{\circ}$, is considered on the basis of the discovery[2] from experiment that an analysis of the flow at a constant angle of incidence yields an understanding of the nature of the flow both at a given angle of incidence, and at maximum lift. A range of values of flap gaps is examined, the most detailed analysis being performed for those cases in which it is possible to distinguish between the wake of the main aerofoil and the flap boundary layer. Overlap is held constant at 4% of the wing basic chord.

Where possible, experimentally-derived results[5] for the development of the aerofoil wake and the flap boundary layer are employed. This approach is adopted in order to remove, as far as possible, any uncertainties resulting from the use of an approximate theoretical method for completing the viscous part of the calculation.

The method used in this investigation has been discussed in detail in Ref.6 and here only a brief outline of the theory is given.

4.2 Flap boundary layer

In order to answer the first of the questions posed in section 4.1 it is necessary to calculate both the effect of the flap boundary layer and of the aerofoil wake on the lift. Here the method used to determine the influence of the flap boundary layer is described.

In Ref.6 it is shown that the flap boundary layer may be simulated by distributions of sources and vortices around the contour c defining the edges of the flap boundary layer and the flap wake, together with a vortex distribution on the surface of the aerofoil. This representation may be simplified considerably by assuming that:

(a) the aerofoil and the flap are both of small thickness - chord ratio and camber;

(b) the flap angle is small;

(c) the flap gap and overlap are small; and

(d) the boundary layer and the wake of the flap are both thin compared with the flap chord.

These assumptions lead to the model shown in Fig.9 by which the singularities are placed on the chord of the main aerofoil and its downstream extension. This model clearly represents a radical simplification of the physical situation but, for the present purpose of conducting a comparative analysis of viscous effects, it is considered to be adequate. It might be argued that the neglect of the gap effect in this model could result in serious errors in the viscous corrections to the lift. However, inviscid calculations[5] indicate that the change in lift resulting from a change of flap gap is small compared with the total lift in the range of values of flap gap examined.

The local strength of the vortex distribution associated with the flap boundary layer, $\Delta\gamma_{,B}$, is determined[6] by satisfying the requirement that there is no flow normal to the chord of the main aerofoil and by observing that the flap boundary layer effectively increases the ζ-component of velocity, v_ζ, at the flap chord by the amount

$$(\Delta v_\zeta)_{,B} = \frac{1}{2}\left(\frac{d(U_u \delta^*_u)}{d\xi} - \frac{d(U_L \delta^*_L)}{d\xi}\right) \quad . \tag{1}$$

Here δ^* = displacement thickness of flap boundary layer;

U = speed of flow at edge of boundary layer;

(ξ,ζ) = rectangular, cartesian coordinate system, ξ axis along aerofoil chord, $\xi = 0$ at aerofoil leading edge;

suffixes u,L refer to upper and lower surfaces of flap.

Hence, upon satisfying these boundary conditions, it is found that

$$\frac{1}{2\pi}\int_0^\infty \Delta\gamma_{,B}(\xi')\,\frac{d\xi'}{\xi - \xi'} = \begin{cases} \frac{1}{2}\frac{dF}{d\xi}, & \xi \geqslant c_A ; \\ 0, & 0 \leqslant \xi < c_A . \end{cases} \tag{2}$$

where c_A is the chord of the main aerofoil and

$$F = U_L \delta^*_L - U_u \delta^*_u \quad . \tag{3}$$

For the purpose of evaluating the vortex strength it is convenient to regard the wake of the flap as part of the wake of the main aerofoil. This would seem intuitively to be an acceptable way of proceeding since the two wakes tend to merge downstream of the flap, and in this region it is difficult to distinguish one wake from the other. Therefore discussion of the wake vortex effect is deferred until section 4.3 wherein the effect of the aerofoil wake is examined, and, for the time being, it is supposed that

$$\Delta\gamma_{,B}(\xi) = 0 , \quad c_E < \xi \leq \infty , \tag{4}$$

where c_E is the chord of the wing when the flap is deployed. The resulting integral equation can be inverted in the manner described by Weber[7], and this inversion is rendered unique by satisfying the requirement, derived from physical considerations[6], that $\Delta\gamma_{,B}$ is finite at $\xi = c_E$. Consequently

$$\Delta\gamma_{,B}(\xi) = \frac{1}{\pi}\left(\frac{c_E - \xi}{\xi}\right)^{\frac{1}{2}} \int_{c_A}^{c_E} \left(\frac{\xi'}{c_E - \xi'}\right)^{\frac{1}{2}} \frac{dF}{d\xi'} \frac{d\xi'}{\xi' - \xi} . \tag{5}$$

The local strength of the source distribution, $\Delta q_{,B}$, follows from the fact that the flap boundary layer effectively induces the jump in the ζ-component of velocity across the flap chord

$$[(\Delta v_\zeta)_{,B}]_u - [(\Delta v_\zeta)_{,B}]_L \equiv \Delta q_{,B} = \frac{d(U_u \delta_u^*)}{d\xi} + \frac{d(U_L \delta_L^*)}{d\xi} . \tag{6}$$

Thus, with the local strengths of the source and vortex distributions determined, the influence of the flap boundary layer on the velocity distribution external to the flap boundary layer may be established. With this information, and by using Bernoulli's equation, it is possible to evaluate the pressure distribution around contour c. In order to relate the pressures at the edge of the flap boundary layer to the pressures at the surface of the flap use is made of Prandtl's boundary-layer approximation in which the rise in pressure across the boundary layer is ignored. Strictly, this approximation fails in regions where the mean radius of curvature of the streamlines is small compared with the reference chord. An obvious example of such a region is the neighbourhood of the trailing edge of the flap. However, measurements[5] reveal that the variation

of static pressure across the boundary layer is generally small compared with the change in pressure associated with the displacement effect of the boundary layer. Thus, upon resolving the pressure forces in the direction of the lift, it is found that the increment in the lift of the flap due to the boundary layer is, to the order of approximation of the present theory, given by[6]

$$\Delta L_{F,B} = \rho \cos(\beta + \alpha) \int_{c_A}^{c_E} \left\{ (U_I)_u [(\Delta v_\xi)_{,B}]_u - (U_I)_L [(\Delta v_\xi)_{,B}]_L \right\} d\xi \quad , \qquad (7)$$

with v_ξ the ξ- component of velocity. Here U_I, which is the speed of the flow on the flap according to the first inviscid approximation, is obtained by using the Douglas-Neumann numerical method[8].

The increment in total lift due to the flap boundary layer, $\Delta L_{,B}$, follows from application of the lift-circulation theorem[9] *viz*:

$$\Delta L_{,B} = \rho V_\infty \int_0^{c_E} \Delta\gamma_{,B} d\xi \quad , \qquad (8)$$

with V_∞ the free-stream speed.

4.3 Wake of main aerofoil

4.3.1 Approximation for thin wake

As in the case of the flap boundary layer it is possible to represent the influence of the vorticity of the wake of the main aerofoil on the flow by distributions of sources and vortices around the contour defining the extremes of the wake[6] (see Fig.10a). In Ref.6 it is shown that, for a sufficiently 'thin' wake, these distributions may be replaced by distributions of sources and vortices on a suitable mean line of the aerofoil wake together with a point source placed at the shroud trailing edge. This representation is illustrated in Fig.10b. The point source arises from the neglect of the boundary layer of the main aerofoil. Its rôle is to provide the step in displacement thickness at the shroud trailing edge that is necessary to yield a non-zero displacement thickness in the wake of the main aerofoil. With the inclusion of the boundary layer of the main aerofoil the point source is replaced by a distribution of sources along the edge of the boundary layer. Simple continuity considerations

show that the integrated strength of these sources is equal to the strength of the point source. The point source may therefore be regarded as an approximation to the distributed sources of the boundary layer of the main aerofoil. Also associated with the existence of a boundary layer on the main aerofoil is an additional distribution of vortices on the aerofoil chord. These are required to cater for the effective change in the camber of the main aerofoil that is caused by the aerofoil boundary layer. This effect is neglected in the present study because the aim is to establish the effect of the wake of the main aerofoil compared with the influence of the flap boundary layer. In fact, as will be seen in section 5, the camber effect of the boundary layer of the main aerofoil appears to be of relatively minor importance.

A further simplification, leading to the model of Fig.10c, can be achieved by making use of assumptions (a), (b) and (c) of section 4.2. In this model the sources and vortices are placed on the ξ axis which is supposed to be situated at a constant height z_T above the flap chord. Consistency with the model of Fig.9 is assured if the condition that $z_T/c_F \ll 1$ is imposed, where c_F is the flap chord. With this condition it is readily found that the ζ- component of velocity induced by the wake at the combined aerofoil-flap chord is, to a first approximation, given by

$$(v_\zeta)_i = \frac{1}{2\pi}\int_{c_A}^{\infty} \gamma_W \frac{d\xi'}{\xi' - \xi} - \frac{1}{2}\frac{d(U_W\delta_W^*)}{d\xi}$$

$$- \frac{1}{2\pi} U_W(c_A)\delta_W^*(c_A) \frac{z_T}{(\xi - c_A)^2 + z_T^2}, \quad \xi > c_A \ . \qquad (9)$$

Here

$$\gamma_W = (\Delta v_x)_+ - (\Delta v_x)_- \qquad (10)$$

is the wake vortex strength, with v_x the x-component of velocity and (x,z) the rectangular, cartesian coordinate system with the x axis along the flap chord and $x = 0$ at the flap leading edge. Suffixes $+$ and $-$ refer to the upper and lower edges of the wake at any station x. Additionally,

$$U_W = \tfrac{1}{2}[(v_x)_+ + (v_x)_-] \ , \qquad (11)$$

that is the mean of the x-components of the velocities at the upper and lower edges of the wake, and δ^*_W is the wake displacement thickness.

It will be seen that, in this approximation, the wake vortices are effectively transferred to the flap chord and its downstream extension. As well it will be noted that the upwash induced by the distributed sources (the second term on the right-hand side of equation (9)) depends only on the local strength of the sources, in consequence of the assumption that they lie just above the flap chord. Finally, it should be remarked that the last, or point-source term of equation (9) has not been approximated for small z_T/c_F; the reason for this is that this approximation evidently fails for $\xi = c_A$.

It may be shown[6] that, for a 'thin' wake that is either close to or substantially parallel with the flap chord

$$\gamma_W = \kappa_W U_W(\delta^*_W + \theta_W) \quad . \tag{12}$$

Here κ_W = weighted mean curvature of streamlines of wake[6], the centre of curvature being taken below the wake; and

θ_W = wake momentum thickness.

To ensure that the main aerofoil and the flap remain streamlines in the presence of the wake an additional vortex distribution is required on the line representing the combined chord of the aerofoil and the flap. This condition leads to the integral equation for the strength of this vortex distribution, $\Delta\gamma_{,W}$, namely,

$$\frac{1}{2\pi}\int_0^{c_E} \Delta\gamma_{,W}(\xi')\,\frac{d\xi'}{\xi - \xi'} = \frac{1}{2\pi}\int_{c_A}^{\infty} \gamma_W\,\frac{d\xi'}{\xi' - \xi} - \frac{1}{2}\,\frac{d(U_W\delta^*_W)}{d\xi}$$

$$- \frac{1}{2\pi}\,U_W(c_A)\delta^*_W(c_A)\,\frac{z_T}{(\xi - c_A)^2 + z_T^2}\,, \qquad \xi > c_A \quad . \tag{13}$$

It is interesting to compare this expression with equation (2). This comparison reveals that, if the wake vortices are neglected, the wake effect is, to the order of the present approximation (in which U_W is substantially equal to U_u), equivalent to an increase in the displacement thickness of the boundary layer of

the flap upper surface by the amount δ_W^* , except in the immediate vicinity of the shroud trailing edge. A calculation method that employs this approach in conjunction with the Douglas-Neumann computer program is described in section 5.

In section 4.2 it was supposed that, for the purpose of evaluating the vortex effect, the wake of the flap is regarded as a vertical extension of the wake of the main aerofoil. With this assumption γ_W becomes the vortex strength of the combined wake for points downstream of the flap trailing edge.

Equation (13) is inverted in the manner used to invert equation (2). Uniqueness of this inversion is assured by observing that, according to the present approximation, $\Delta\gamma_{,W}$ is the wake contribution to the jump in tangential velocity between two adjacent field points on the contour c. That is to say $\Delta\gamma_{,W}$ is required to be finite. Thus, upon performing the inversion and by making use of an integral identity given by Spence[10], it is found that[6]

$$\Delta\gamma_{,W}(\xi) =$$

$$= -\gamma_W + \frac{1}{\pi}\left(\frac{c_E - \xi}{\xi}\right)^{\frac{1}{2}} \int_{c_E}^{\infty} \left(\frac{\xi'}{\xi' - c_E}\right)^{\frac{1}{2}} \gamma_W \frac{d\xi'}{\xi' - \xi}$$

$$- \frac{1}{\pi}\left(\frac{c_E - \xi}{\xi}\right)^{\frac{1}{2}} \int_{c_A}^{c_E} \left(\frac{\xi'}{c_E - \xi'}\right)^{\frac{1}{2}} \left\{ \frac{d(U_W \delta_W^*)}{d\xi'} + \frac{1}{\pi} U_W(c_A)\delta_W^*(c_A) \frac{z_T}{(\xi' - c_A)^2 + z_T^2} \right\} \frac{d\xi'}{\xi' - \xi} ,$$

$$\xi > c_A \quad . \qquad (14)$$

The last integral of equation (14), in common with the integral of equation (5), is evaluated numerically without difficulty[6]. To evaluate the first integral of equation (14) use is made of the analogy between the jet sheet of an internal-flow jet flap and the wake downstream of a wing with a flap. Full details of this procedure are given in Ref.6.

4.3.2 Effect of wake thickness

In this section consideration is given to the second of the questions posed in section 4.1, namely the question of the significance of wake thickness. Additionally, the effect of the distance of the wake from the flap is examined.

In Ref.6 it is shown that, after a first-order correction for wake thickness and distance of the wake from the flap is applied, equation (9) may be rewritten as

$$(v_\zeta)_i = \frac{1}{2\pi}\int_{c_A}^{\infty} \bar{\gamma}_W \frac{d\xi'}{\xi' - \xi} - \frac{1}{2}\frac{d(U_W\bar{\delta}^*_W)}{d\xi} - \frac{1}{2\pi} U_W(c_A)\delta^*_W(c_A)\frac{z_T}{(\xi - c_A)^2 + z_T^2}, \quad \xi > c_A \quad . \quad (15)$$

That is to say the displacement thickness δ^*_W in the distributed-source term is replaced by the effective displacement thickness

$$\bar{\delta}^*_W = \delta^*_W + \gamma_W^{(1)}(z_+ + z_-)/2U_W \quad , \quad (16)$$

with z_+ and z_- the z ordinates of the upper and lower edges of the wake, respectively, and $\gamma_W^{(1)}$ a first approximation to the vortex strength γ_W given by equation (12). As well, the vortex strength is altered to

$$\bar{\gamma}_W = \gamma_W^{(1)} - \frac{1}{2}\frac{d^2(U_W\delta^*_W)}{dx^2}(z_+ + z_-) \quad , \quad (17)$$

for a wake that is substantially parallel to the flap chord.

Hence the last terms in equations (16) and (17) may be regarded as correction terms for nonzero wake thickness and for the distance of the wake from the flap chord. However, if the distance of the wake from the flap chord is defined in terms of the z ordinate of the mean line of the wake

$$z = (z_+ + z_-)/2 \quad (18)$$

the corrections do not depend on wake thickness. That is to say, if the position of the wake mean-line is known, it is only necessary to correct the results of section 4.3.1 for the distance of the wake from the flap.

Equation (18) implies that the effective or apparent increase in circulation in the part of the wake that is downstream of the flap, arising from the thickness-distance correction, is given by

$$\Delta\Gamma = -\frac{1}{2}\int_{c_F}^{\infty} \frac{d^2(U_W\delta_W^*)}{dx^2}(z_+ + z_-)dx \quad . \tag{19}$$

Therefore, upon using the assumption that the second derivative of $U_W\delta_W^*$ decays rapidly downstream of the trailing edge of the flap, equation (19) may be approximated as

$$\Delta\Gamma = \frac{1}{2}\left|\frac{d(U_W\delta_W^*)}{dx}(z_+ + z_-)\right|_{x=c_F} \quad . \tag{20}$$

The incremental velocities associated with this change in circulation are determined by equating these velocities to the corresponding velocities of a jet-augmented flap, of the same flap chord, the jet sheet of which has the circulation $\Delta\Gamma$. In Ref.6 an additional allowance is included for the change in circulation in the wake downstream of the flap due to the effect of viscosity on the wake curvature, which effect is neglected in the 'thin' wake method.

4.3.3 Influence of wake on lift

The derivation of the incremental lift acting on the flap due to the wake is identical to the method used to obtain the increment due to the flap boundary layer (equation (7)). For a 'thin' wake, the resulting expression is similar to equation (7) except that $(\Delta v_\xi)_{,B}$ is replaced by $(\Delta v_\xi)_{,W}$, *viz*:

$$\Delta L_{F,W} = \rho\cos(\beta+\alpha)\int_{c_A}^{c_E}\left\{(U_I)_u[(\Delta v_\xi)_{,W}]_u - (U_I)_L[(\Delta v_\xi)_{,W}]_L\right\}d\xi \quad . \tag{21}$$

If the distance of the wake from the flap is 'small' it is possible to make use of the approximate method of section 4.3.1 to determine $[(\Delta v_\xi)_{,W}]$. The effect of thickness-distance is included by using the method of section 4.3.2. However, to proceed to higher-order approximations for $\Delta L_{F,W}$, it may not be sufficient to replace the incremental velocities in equation (21) by their higher-order equivalents. The reason for this is that the terms neglected in deriving equation (21) may be of the same order of magnitude as the correction

to $[(\Delta v_\xi)_{,W}]$, for the effect of the thickness of the wake. Thus, strictly, when including the effect of non-zero thickness it is necessary to include squares and products of the correction terms. In practice, it is found that the additional terms have only a slight effect on the wake correction to flap lift.

As with the flap boundary layer, the increment in total lift due to the wake is determined by means of the lift-circulation theorem[9]; in this case, however, when evaluating the increment in total circulation, not only the vortices on the ξ axis are included but also the vortices in the wake of the main aerofoil.

4.4 Calculations

4.4.1 Flap boundary layer

As noted before, the calculations have been mainly based on measured boundary-layer and wake properties. Fig.11 shows typical distributions of displacement thickness, δ^*, of the flap boundary layer for the two flap gaps, 2% and 4%. It is seen that the upper-surface distributions were deduced from measurements whilst, in the absence of velocity surveys in the lower layer, the lower-surface distributions were calculated[6].

By using equation (1) and noting that to the order of the present approximation

$$U_u = U_L = V_\infty \tag{22}$$

it is readily shown that the effect of the flap boundary layer is equivalent to an upward displacement of the camber line of the flap by the amount

$$\tfrac{1}{2}(\delta^*_u - \delta^*_L) \quad .$$

Hence, by examining Fig.11 it may be concluded that the flap boundary layer induces a significant decrease in the effective camber of the flap particularly near to the flap trailing edge. This is of some importance since linearized aerofoil theory[9] indicates that total lift is most sensitive to changes in the slope of the camber line in this region.

The effect of the flap boundary layer on both the flap lift and the total lift, as calculated by the method of section 4.2 is illustrated in Fig.12. This figure shows the two lift components plotted against flap gap. The first inviscid approximation (curve (a)) evidently overestimates the total lift and

the flap lift by a significant margin in either case, whereas inclusion of the effect of the flap boundary layer (curve (b)) results in a noticeable improvement in agreement between theory and experiment. Note that curve (b) is restricted to flap gaps above 2%, in consequence of the fact that the flap boundary layer and the aerofoil wake are indistinguishable for flap gaps below this value.

4.4.2 Aerofoil wake

The curve (c) in Fig.12 is the curve (b) with the wake effect added in accord with the method of section 4.3.1, i.e. for a 'thin' wake that is 'close' to the flap. It should be noted that curve (c) is continued below a gap of 2% despite the fact that, for gaps below this value, it is impossible to distinguish between the boundary layer and the aerofoil wake, at least over part of the flap chord. Nevertheless, the combined effect of the two layers can still be determined by the above mentioned method even though the boundary between the 'wake' and the 'boundary layer' has to be chosen arbitrarily. In fact, it may be shown that the total lift is independent of the choice of dividing line, and, for a gap of 0.5%, the flap lift is found to be insensitive to changes in the position of this line. It is interesting to record that the present method correctly predicts the optimum gap for total lift. In view of the approximations involved this is perhaps surprising; but it is worth noting that the optimum given by the present method owes its existence to the large decrease in the chordwise slope of the effective camber line of the flap near to the flap trailing edge, resulting from the separation of the flow from the flap upper surface, which occurs for gaps of less than 1%.

One of the most significant conclusions to be drawn from Fig.12 is that the wake effect predicted by the present method is small compared with that due to the flap boundary layer. This provides the answer to the first of the questions posed in section 4.1. The reason for the relative smallness of the wake effect can be established by referring to Figs.13a and b. Fig.13a, in particular, shows plots of $U_W\delta^*_W/V_\infty c_o$ against x/c_o for the two flap gaps 2% and 4%, c_o being the chord of the basic wing. Now, to a good approximation, and consistent with equation (22)

$$U_W = V_\infty \ ;$$

and, as noted before, the sources of the wake have the same effect as an increase in the displacement thickness of the boundary layer of the flap upper surface by the amount δ^*_W. Thus, by comparing Figs.11 and 13a, it may be inferred that the effect of the distributed sources on both the total lift and the flap lift is small compared with that due to the flap boundary layer, the chordwise slope of the effective camber, induced by the distributed sources, at the flap trailing edge being small compared with the corresponding slope induced by the flap boundary layer. Similarly, as may be deduced from Fig.13a and equation (9), the effect of the point source on the lift is small since the change of angle of incidence it induces at the flap trailing edge is small.

Fig.13b shows the vortex strength $\gamma_W^{(1)}/V_\infty$ plotted against x/c_0 for the part of the aerofoil wake that is above the flap and for the two flap gaps 2% and 4%. The effect of these vortices on the total lift is exactly cancelled by an equal and opposite distribution of vortices on the flap chord, the latter distribution being required to nullify the downwash induced by the vortices of the aerofoil wake. Consequently only the vortices representing the combined wake downstream of the flap contribute to the total lift, and it is found that these vortices are responsible for approximately half the wake correction. In the case of the flap lift it may be deduced from Fig.13b that, for the 2% gap, the combined effect of the wake vortices just above the flap and the equal and opposite vortex distribution on the flap chord is to produce a slight increment in the flap lift. This explains why, in this case, the wake correction to flap lift, as a percentage of flap lift, is smaller than the corresponding correction to total lift is as a percentage of total lift.

Fig.14 shows the effect of including the thickness-distance correction in the wake contribution (curve (d)). In the case of the total lift the thickness-distance correction has little effect for a gap of 4%, whereas, close to the optimum gap, its application results in a significant increase in the lift. The thickness-distance correction also produces a small increase in the flap lift. Indeed, for a gap of 2%, the increment due to this correction completely offsets the decrement arising from the first approximation to the wake effect. The cause of this may be identified with the fact that, in the first approximation, the major part of the wake effect comes from the distributed sources. As is shown in Fig.15 for a flap gap of 2%, when the thickness-distance correction is included, the effective displacement thickness of the aerofoil wake is significantly reduced near to the flap trailing edge with a consequent reduction in the adverse

camber induced by the sources there. As may be inferred from equation (16) the change in the effective displacement thickness is directly attributable to the vortices $\gamma_W^{(1)}$ which, for the 2% gap, assume particular significance in the region of the flap trailing edge. For the 4% gap, on the other hand, $\gamma_W^{(1)}/V_\infty$ is very small in this region. This explains why the thickness-distance correction to total lift is small for the 4% gap.

Since the thickness-distance correction is such a large proportion of the wake effect it is worth enquiring whether the second, or corrected, approximation is particularly accurate. An examination of the integrals for the velocity induced by a 'thick' wake indicates that the second approximation is of acceptable accuracy for the wake geometries examined here if $U_W\delta_W^*/V_\infty c_o$, $\gamma_W^{(1)}/V_\infty$ and the various derivatives of these functions with respect to x/c_o are at most $O(1)$ uniformly along the wake. As may be seen by examining the experimental results, this proviso appears to be satisfied for the part of the wake above the flap.

4.5 Interim conclusions

It is worth summarizing the main conclusions of this part of the Report. These are as follows:

(i) The effect of the wake on the lift is small compared with that due to the flap boundary layer, at least for the flap configuration studied here.

(ii) If the distance of the wake from the flap is defined in terms of the z ordinate of the mean line of the wake, the wake thickness corrections to the effective vortex and source strengths vanish.

(iii) The thickness-distance correction to the wake effect yields an increment in lift which is a large proportion of the total wake effect. However, since the wake effect is small, the errors obtained by ignoring this correction are also small.

5 REPRESENTATION OF VISCOUS EFFECTS FOR MULTIPLE AEROFOILS

5.1 Introductory remarks

In section 4 it was shown that, for the purpose of calculating lift, the wake of the main aerofoil of a two-element aerofoil is of secondary importance compared with the boundary layer of the flap, and thus there is some justification for using an approximate method of including the effect of the aerofoil

wake. However, whilst the method of section 4 can be used to examine the relative importance of viscous effects, it is not suitable for routine application. What is required instead is a procedure based on a well-established method for calculating potential flows around multiple aerofoils. For some years the Douglas-Neumann method[8] appears to have found most favour both in industry and research establishments, although, only recently has it been demonstrated[11] that it is capable of yielding an accurate potential-flow solution for multiple aerofoils.

In order to account for the viscous layers use is made here of an extension of the well-known principle that a boundary layer effectively displaces the inviscid flow outwards by the displacement thickness of the layer. In general, the displacement surface of each element of a multiple-element aerofoil is defined totally by the displacement thickness of the boundary layer, provided that there exists a region of inviscid flow between the boundary layer and the wake of the upstream element. Where there is no inviscid flow between the two layers, the displacement surface is defined by the displacement thickness of the combined layer. If this definition is followed rigorously then there is a discontinuity in the displacement surface at the point where the region of inviscid flow terminates. To overcome this difficulty a smooth displacement surface is faired in over a small region, upstream of this point, so that it fits between the displacement surface of the boundary layer and the displacement surface of the combined wake and boundary layer. The model implied by this treatment is shown in Fig.16, and it is seen that, since the displacement thickness at the trailing edge of each element is non-zero, the resulting displacement surface is not closed. However, it is still possible to calculate the flow about this profile by using the Douglas-Neumann method.

Insofar as the present method allows for the displacement effect of the 'wake' when the two layers begin to merge it is similar to the method of section 4.3.1. On the other hand, unlike the method of section 4.3.1 no allowance is made either for the wake vortex effect or for the sink effect of the wake upstream of the place where the two layers start to join. However, since the wake effect is of secondary importance it is considered that the error resulting from the neglect of these effects is probably small.

For the thick viscous layer over the flap, some care must be taken with the calculation of the displacement thickness. It was noted in some recent wind tunnel tests that there is a variation of static pressure through this

layer, and so the definitions of displacement thickness given by Myring[12] have been used to take account of this feature. In some of the examples an attempt has been made to deal with partially separated flows; the displacement thickness in the separated region being extrapolated from the measured or calculated displacement thickness in the region of attached flow.

It will also be shown that the displacement correction, when applied only to the last element, is the dominant factor in determining the lift. The presence of the viscous layer has, of course, two major effects upon the aerofoil; to change the camber distribution and the thickness distribution. Both of these changes are found to be adequately represented by a displacement correction to the last element of the multiple aerofoil.

5.2 The two-element aerofoil

The concepts described above are illustrated here by considering the flow about the two-element configuration examined in section 4, which it will be recalled comprised a slotted flap at 30° deflection, with the angle of incidence at zero. Experimental traverses through the boundary layer and wake gave the values of the displacement thickness at four positions on the upper surface of the flap. By using these values a displacement surface was defined to replace the upper surface of the flap. From Fig.17 it can be seen that the lift generated by these displacement profiles corresponds reasonably well with the measured experimental values, the optimum gap for highest total lift being correctly predicted.

In the example of Fig.17 for a gap setting of 4% chord, the wake and boundary layer join just upstream of the flap trailing edge, and the displacement surface is defined by the displacement thickness of the boundary layer over most of the flap chord. As the gap decreases, the point at which the layers join moves forward, and for a gap of 2% chord the layers join at the mid-chord position. At a gap of 0.5% chord the wake and boundary layer are joined over the whole surface of the flap and the displacement surface is defined by the combined wake and boundary layer.

In all these cases the boundary layer on the flap separated at about three quarters of the flap chord. The length of separated flow was a minimum for the optimum gap setting.

Measurements of the displacement thickness in the region of attached flow were used to obtain an estimate of the growth of the displacement thickness in

the separated region. This process must be treated with some caution, especially at 0.5% gap, where the separated flow extends over the final 40% of the flap chord. The uncertainty of predicting the growth in the separated region probably accounts for some of the discrepancy between the experimental and calculated values in Fig.17.

5.3 The three-element aerofoil

In this section the method is taken a stage further, to consider the three-element aerofoil shown on Fig.16. Experimental pressure distributions were used to enable more extensive information to be obtained on the development of the viscous layers around the aerofoil, and these results were used to calculate the effect of the viscous layers on the flow around the multiple aerofoil.

5.3.1 Calculation of the development of the viscous layers

The initial development of the boundary layer from the stagnation point is not influenced by the wake from any upstream element of the multiple aerofoil, insofar as the wake and boundary layer are separate. Thus the laminar part of the boundary layer can be calculated by the method due to Thwaites[9], and transition can be predicted by the criterion of Granville[13] or by the reattachment of a laminar separation bubble, following Horton's[14] method. The development of the turbulent part of the boundary layer on the most upstream element (the slat) was predicted by Green's[15] extension of Head's method. As no satisfactory method exists for calculating separated flows, it was assumed that the displacement thickness remained constant on the lower surface, over the remainder of the slat chord. This assumption should not significantly affect the calculation of the viscous correction to the lift on the slat itself, but is obviously inadequate if the subsequent development of the wake/boundary layer interaction is to be calculated by purely theoretical means.

To avoid this inadequacy, the calculation of the development of the wake and boundary layer over the main aerofoil was started with the experimental values measured at $x/c_o = 0.054$, the position of the first traverse. For this configuration the slat trailing edge was at $x/c_o = 0.030$, thus the traverse was close to the trailing edge of the slat. The simultaneous development of the boundary layer and wake was calculated by the momentum-integral method of Irwin[1], as described earlier. The comparison between the measured and calculated values of the displacement thickness was also shown earlier (Fig.7).

A similar procedure was adopted for the calculation over the flap. The calculation was started at $x/c_o = 0.17$ (referred to the flap coordinate system) and the comparison of measured and calculated values was shown on Fig.8.

5.3.2 Calculation of viscous effects

The viscous layers were represented in the calculation of the flow by the displacement surface, as described in section 5.1. In Fig.18, the lift coefficients for the various viscous corrections are compared with experiment and the inviscid calculation. Initially a displacement correction, including the wake of the main aerofoil, was applied only to the flap, and subsequently displacement corrections were applied to all the elements. It is noteworthy that the additional corrections result in only small changes in the reduction of the lift coefficient from its inviscid value, confirming the suggestion that the condition at the trailing edge of the flap, affecting the camber of the total aerofoil, is the most important feature.

In Fig.19 the pressure distributions for all the elements for each method are compared. The corrections produce good agreement with experimental pressure distributions on the slat and main aerofoil. It is quite plausible that an inviscid solution will contain a small peak at the trailing edge of the main aerofoil, but the trough that precedes this peak is caused by the inability of the inviscid method to deal with a thin trailing edge. The displacement correction to the main aerofoil produces a thick trailing edge and almost removes the trough. However agreement around the leading edge of the flap is not very good. The experimental pressure distribution contains a peak at $x/c_o = 0.06$. This feature is not evident in the pressure distribution for the inviscid solution nor in the solutions with a displacement correction, and it is assumed that the disagreement is caused by the lack of representation of the wake from the main aerofoil in this region.

6 CONCLUSIONS AND FUTURE WORK

The comparisons between the measured development of the viscous layer and that calculated by Irwin's method has shown that this integral method can reasonably predict the development of the viscous layer, starting from experimentally measured properties of the viscous layer. An analysis of the effects of the viscous layer over the flap has been described, and it has been shown that, for the configuration considered here, the effect of the wake from the main aerofoil is small compared with that of the boundary layer. A general

method of incorporating the viscous layers into a calculation of the flow around the complete multiple aerofoil has been considered, and calculations have indicated that the conditions at the trailing edge of the most downstream element have the dominating influence in determining the lift of the multiple aerofoil.

Future developments will lie in the method for calculating the development of the viscous layers, and in the way these layers are represented in a calculation of the flow. A calculation method which is differential in nature is currently being assessed. Its advantage lies in its ability to deal with any velocity profile, and it should be capable of allowing the calculations to commence at the trailing edge of one element and continue to the trailing edge of the next element. The representation of the viscous layers close to the surface by a distribution of sources on the surface of the aerofoil, and of the wakes in the region immediately aft of each element by a distribution of sinks and vortices, is being considered. The Douglas-Neumann method allows the effects of these singularities to be computed without modification to the existing computer program, and it is hoped that the adoption of this method of representation will yield pressure distributions on downstream elements such as the flap which more closely approximate to experimental distributions.

These two future developments will, it is hoped, provide a complete set of methods to enable the viscous flow around the aerofoil section to be calculated by an iterative method, given only the aerofoil profile and the Reynolds number. Extension of this work to three-dimensional conditions will require the development of a method of calculating the inviscid flow around a finite aspect-ratio wing with leading-edge slats and part-span trailing-edge flaps with large deflections, and the development of the three-dimensional equivalent of the calculation method for the viscous flows particular to these configurations. Whilst the bases for these methods exist in methods applicable to plain wings at low-lift conditions, extension to high-lift configurations will inevitably be a lengthy process.

SYMBOLS

c	contour defining edges of flap boundary layer and flap wake
c_A	chord of main aerofoil
c_E	extended chord of wing with high-lift devices deployed
c_F	chord of flap
C_L	total-lift coefficient; $= L/\frac{1}{2}\rho V_\infty^2 c_o$
C_{LF}	flap-lift coefficient; $= L_F/\frac{1}{2}\rho V_\infty^2 c_o$
C_p	static-pressure coefficient
c_o	chord of basic wing i.e. with high-lift devices retracted
F	$= U_L \delta_L^* - U_u \delta_u^*$
L	total lift
L_F	flap lift
q	local source strength
U	speed of flow at edge of flap boundary layer
U_I	first inviscid approximation to speed of flow on flap surface
U_W	mean of x-wise velocities at upper and lower edges of wake
v_x	x-component of velocity
v_ξ, v_ζ	velocity components in ξ and ζ directions
V_∞	free-stream speed
(x,z)	rectangular, cartesian coordinate system, x axis along flap chord, x = 0 at flap leading edge
z_T	height of ξ axis above flap chord (Fig.10)
α	angle of incidence, i.e. angle between chord of basic wing and free-stream velocity vector
β	flap angle
γ	local vortex strength
γ_W	local vortex strength of wake of main aerofoil
$\gamma_W^{(1)}$	first approximation to γ_W for 'thin' wake that is either close to or substantially parallel with the flap chord
$\bar{\gamma}_W$	effective vortex strength of aerofoil wake after application of thickness-distance correction
Γ	circulation
δ^*	displacement thickness
$\bar{\delta}_W^*$	effective displacement thickness of aerofoil wake after application of thickness-distance correction
Δ	incremental part of
κ_W	weighted mean curvature of streamlines of wake[6], centre of curvature being taken below wake

SYMBOLS (concluded)

(ξ,ζ)	rectangular, cartesian coordinate system, ξ axis along chord of main aerofoil, $\xi = 0$ at leading edge of main aerofoil
ρ	density

Suffixes

,B	due to flap boundary layer
i	refers to velocities induced by wake of main aerofoil
u,L	refer to upper and lower surfaces of flap, respectively
,W	due to wake of main aerofoil
+,-	refer to upper and lower edges of wake of main aerofoil

REFERENCES

No.	Author	Title, etc.
1	H.P.A.H. Irwin	A calculation method for the twodimensional turbulent flow over a slotted flap. RAE Technical Report 72124 (ARC 34236) (1972)
2	D.N. Foster H.P.A.H. Irwin B.R. Williams	The twodimensional flow around a slotted flap. ARC R & M 3681 (1970)
3	J.H. Preston	The calculation of lift taking account of the boundary layer. ARC R & M 2725 (1949)
4	D.A. Spence	Prediction of the characteristics of twodimensional aerofoils. J. Aero. Sci., 21, 577 (ARC 15504) (1954)
5	D.N. Foster	Theoretical and experimental results for the RAE 3ft (0.91m) chord model. Unpublished RAE data
6	P.R. Ashill	A study of the effect of the wake of the main aerofoil of a Fowler-flap configuration on the lift of the flap. RAE Technical Report 72081 (ARC 34169) (1972)
7	J. Weber	The calculation of the pressure distribution on the surface of thick cambered wings and the design of wings with given pressure distribution. ARC R & M 3026 (1955)
8	J.L. Hess A.M.O. Smith	Calculation of potential flow about arbitrary bodies. *Progress in Aeronautical Sciences*, Vol.8, 1, 138 Pergamon Press, London (1966)
9	B. Thwaites (ed)	*Incompressible Aerodynamics*. Clarendon Press (1960)
10	D.A. Spence	A treatment of the jet flap by thin-aerofoil theory. RAE Report Aero 2568 (ARC 18472) (1955)
11	B.R. Williams	A comparison of the surface-source solution with an exact solution for the twodimensional inviscid flow about a slotted flap aerofoil. ARC CP No.1214 (1972)

REFERENCES (concluded)

No.	Author	Title, etc.
12	D.F. Myring	The effects of normal pressure gradients on the boundary-layer momentum integral equation. RAE Technical Report 68214 (ARC 30858) (1968)
13	P.S. Granville	The calculation of viscous drag of bodies of revolution. Report No.849 David Taylor Model Basin (1953)
14	H.P. Horton	A semi-empirical theory for the growth and bursting of laminar separation bubbles. ARC CP No.1073 (1967)
15	J.E. Green	Application of Head's entrainment method to the prediction of turbulent boundary layers and wakes in compressible flow. RAE Technical Report 72079 (ARC 34052) (1972)

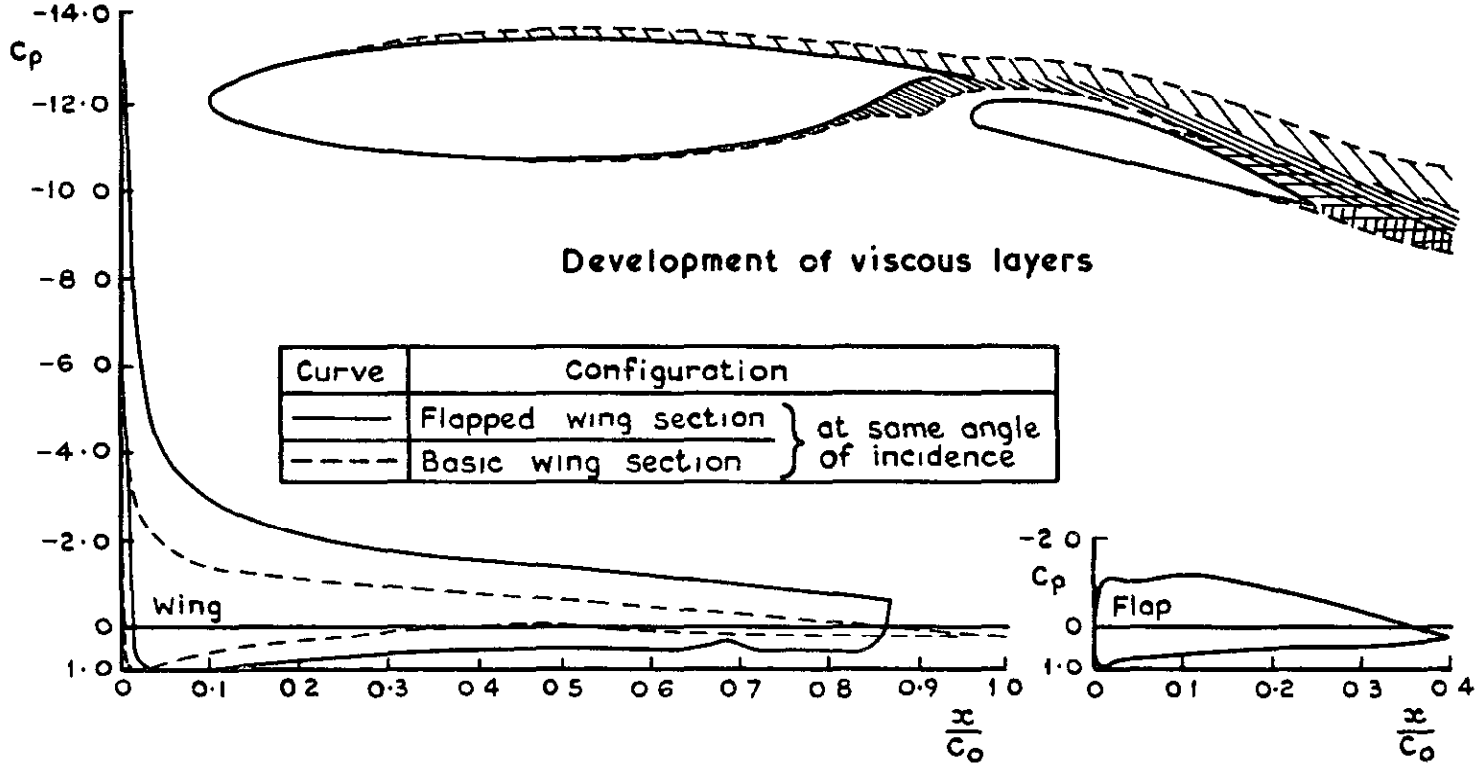

Fig.1 Flow around wing with plain leading edge and slotted flap deflected 20°

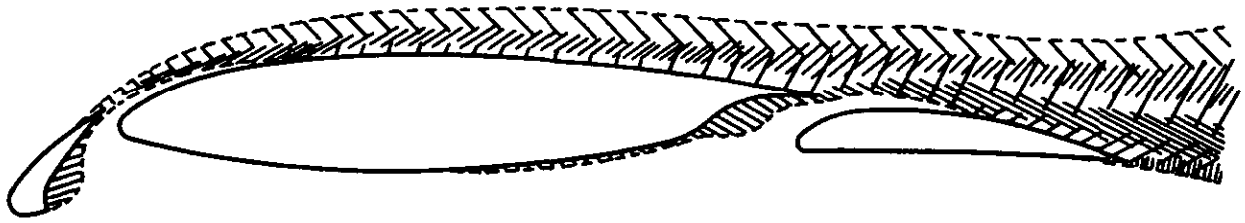

Development of viscous layers

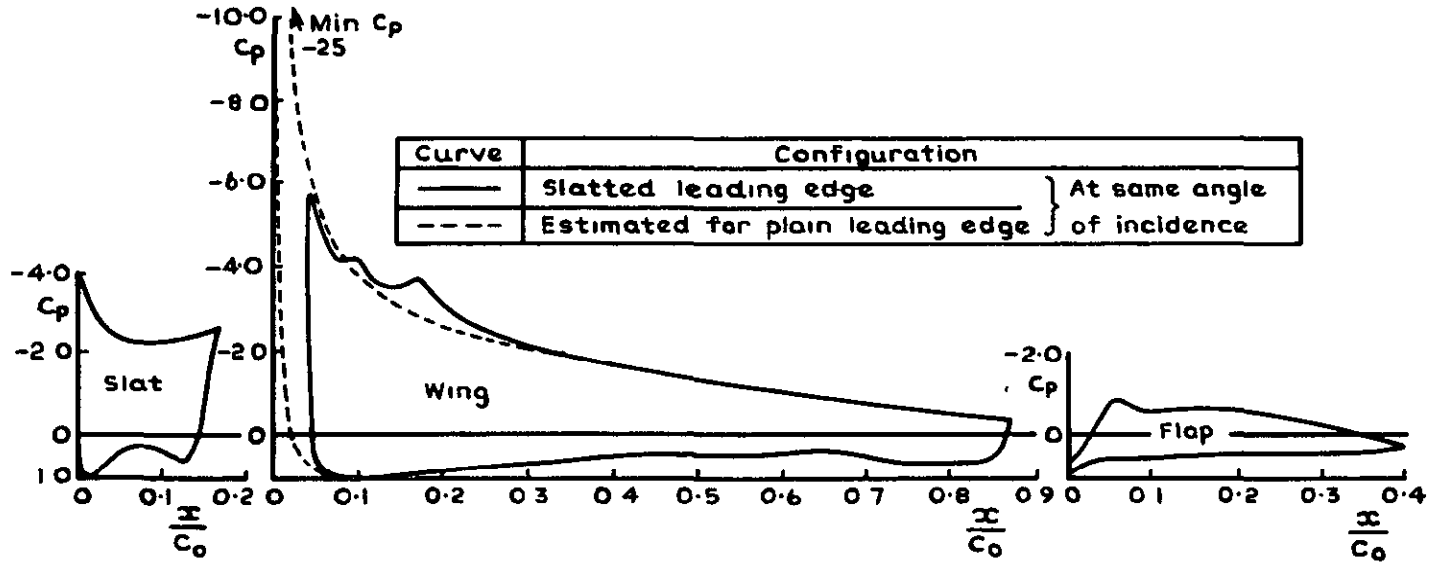

Comparison of pressure distributions

Fig. 2 Flow around wing with slat deflected 28°
and slotted flap deflected 10°

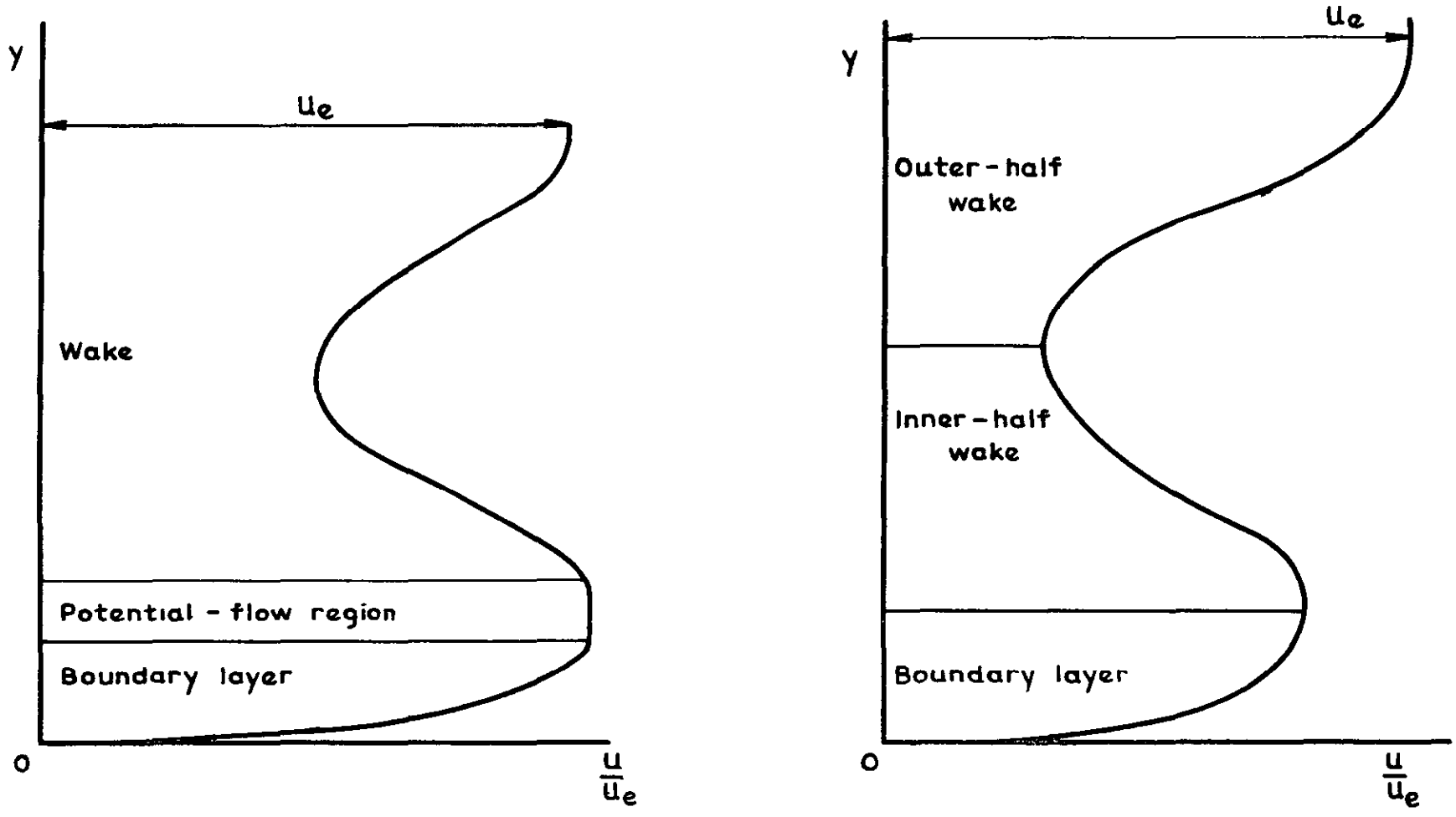

a Wake and boundary layer separate

b Wake and boundary layer merged

Fig. 3a & b Form of velocity profiles

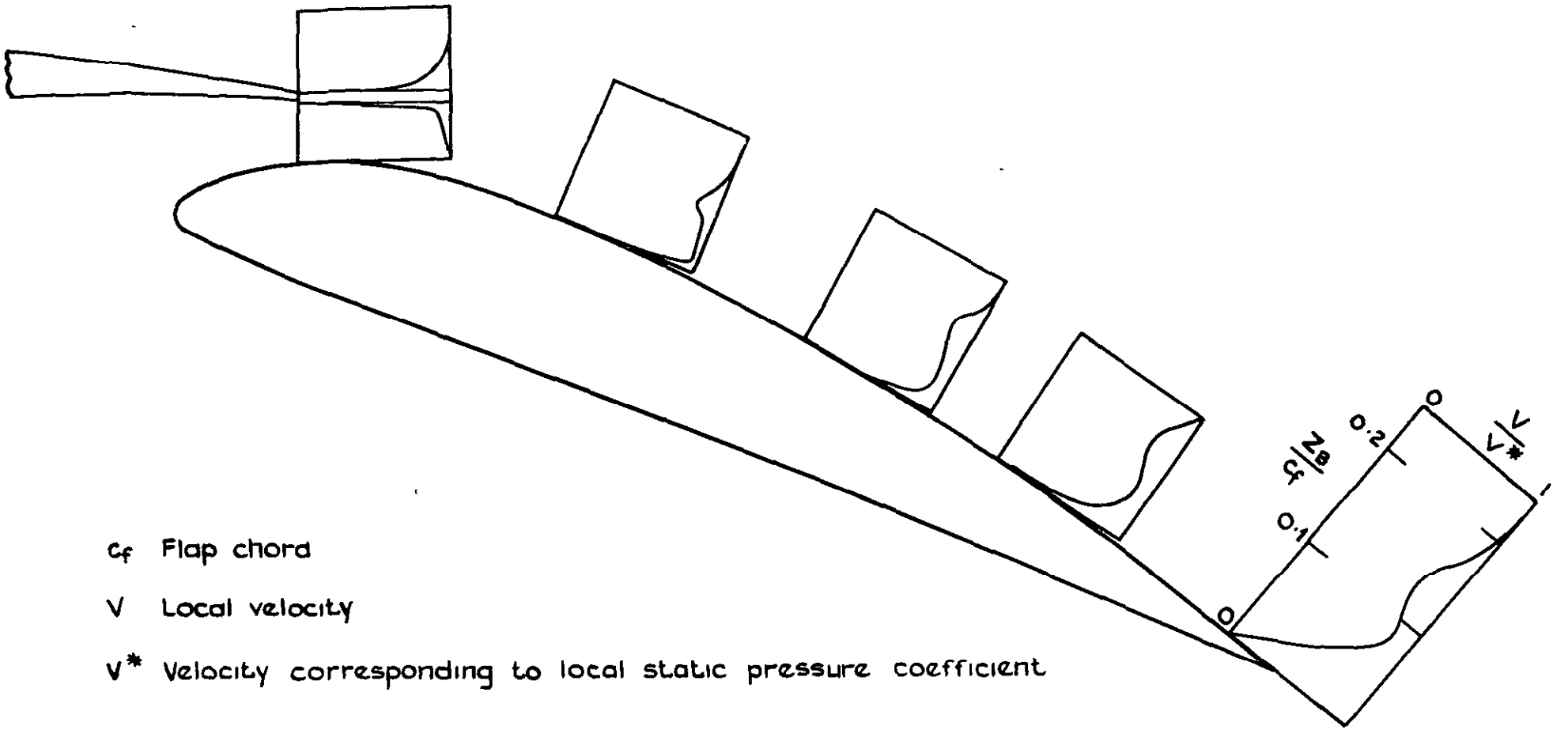

c_f Flap chord

V Local velocity

V^* Velocity corresponding to local static pressure coefficient

Z_B Distance normal to flap upper surface

Fig. 4 Velocity distributions in flow over flap behind plain leading edge

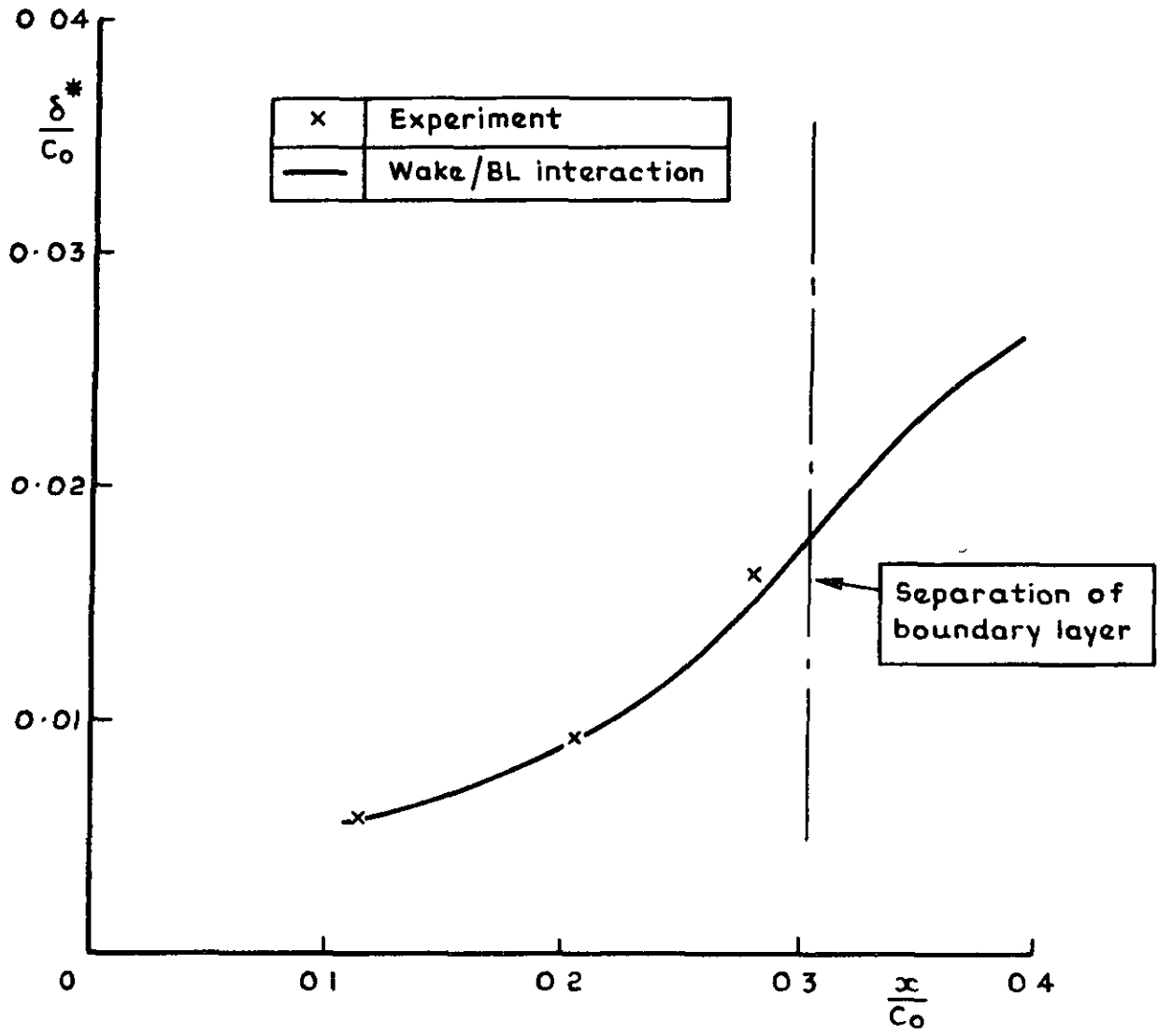

Fig. 5 Development of displacement thickness over flap behind plain leading edge

Fig.5

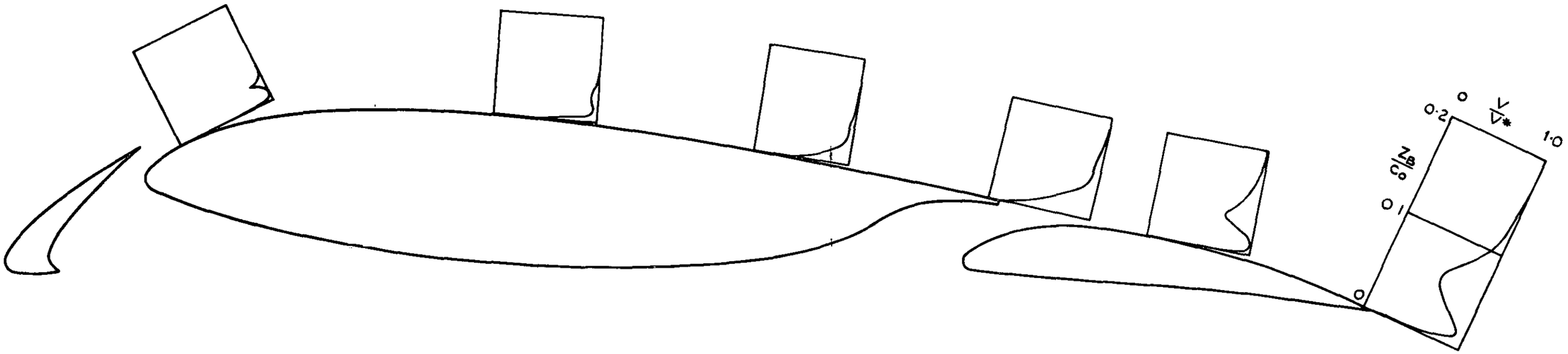

TR 72227

Fig. 6 Velocity distributions in flow over wing and flap behind slatted leading edge

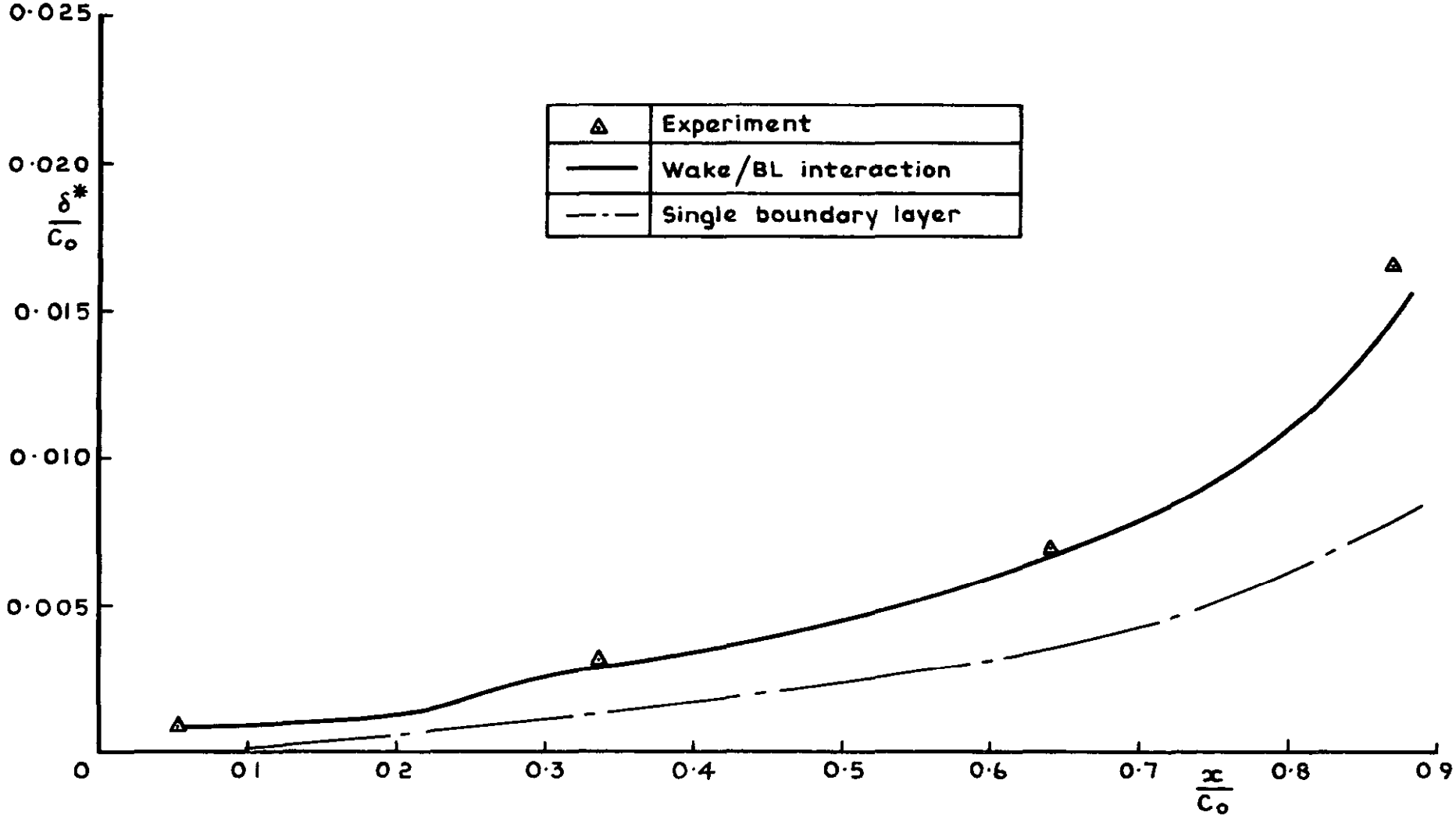

Fig. 7 Development of displacement thickness over main aerofoil behind slatted leading edge

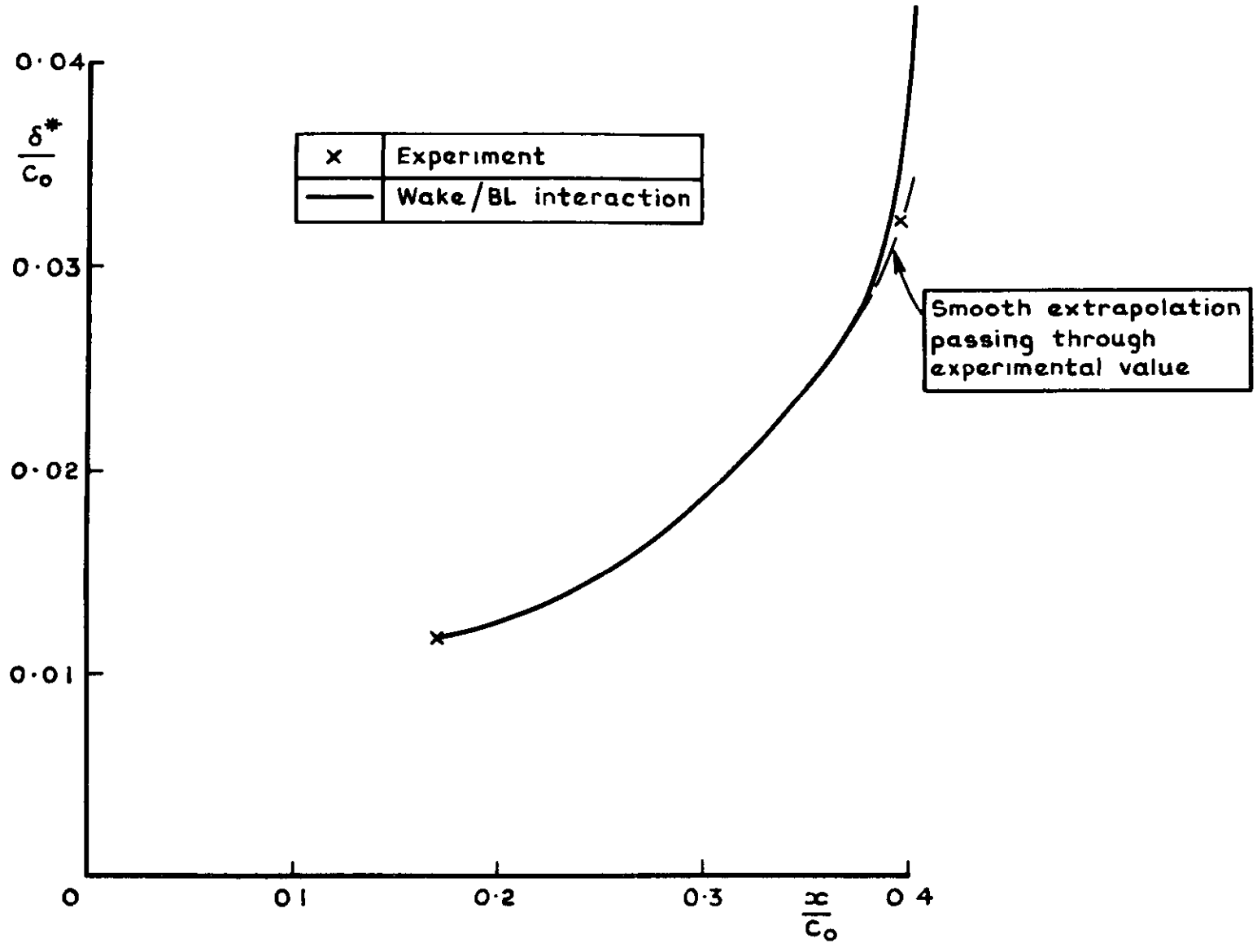

Fig.8 Development of displacement thickness over flap behind slatted leading edge

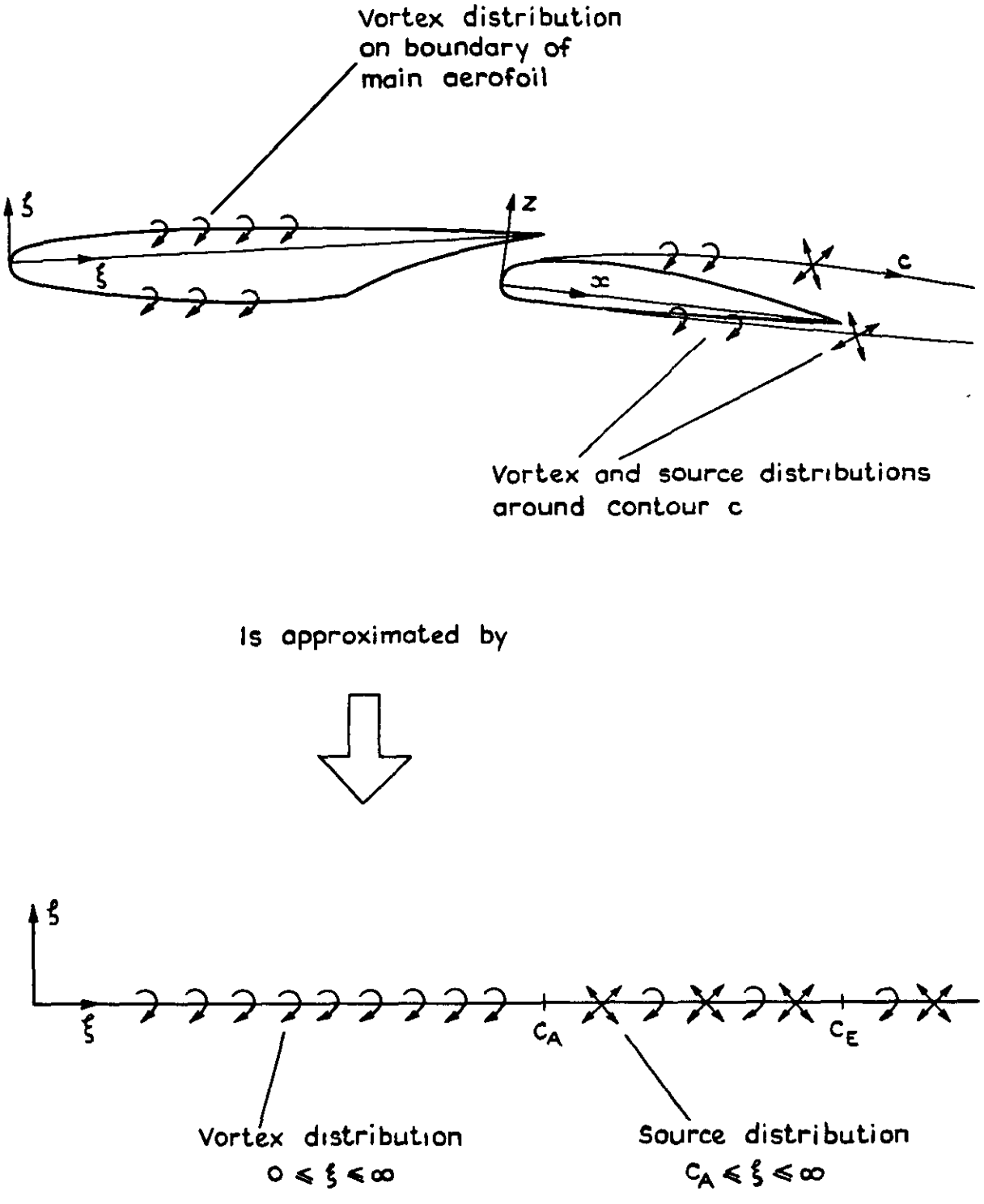

Fig.9 Approximation of vortex and source distributions associated with flap boundary layer

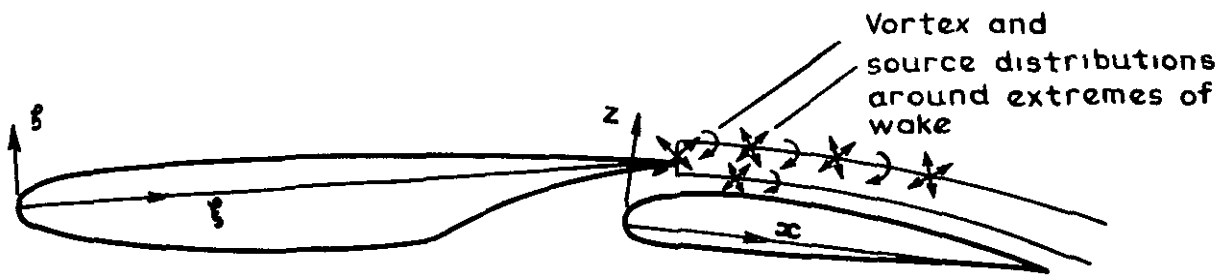

a Thick wake representation

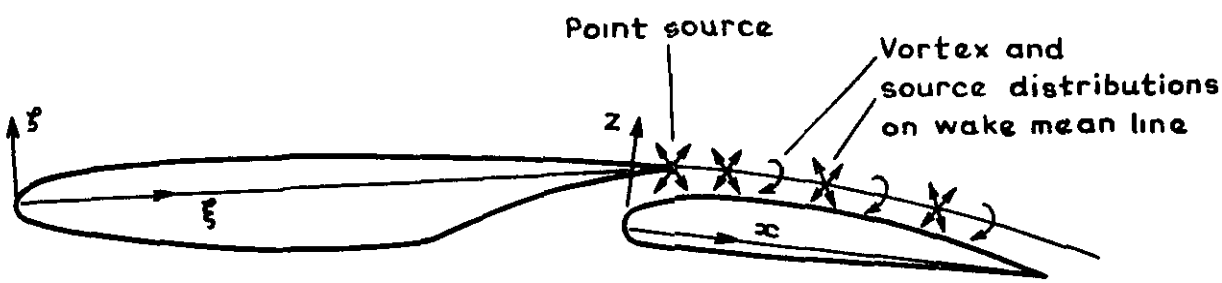

b Thin wake representation

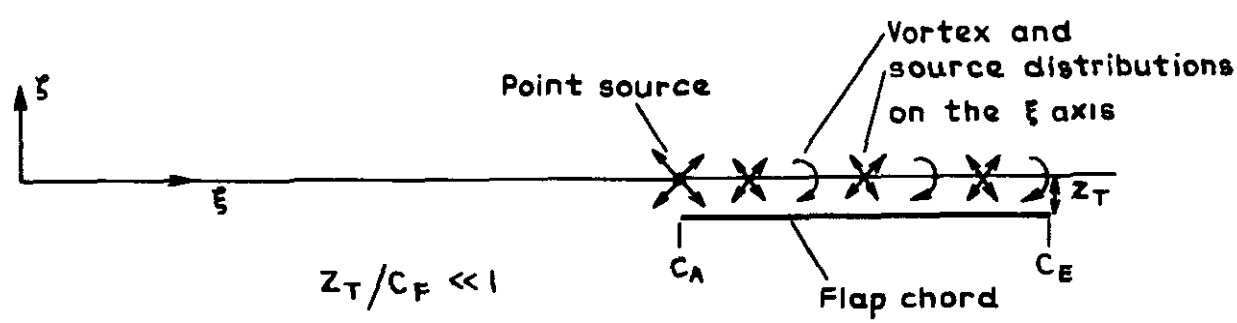

c Thin wake representation for approximate model of Fig. 9

Fig. 10a-c Stages in approximation of source and vortex distributions of aerofoil wake

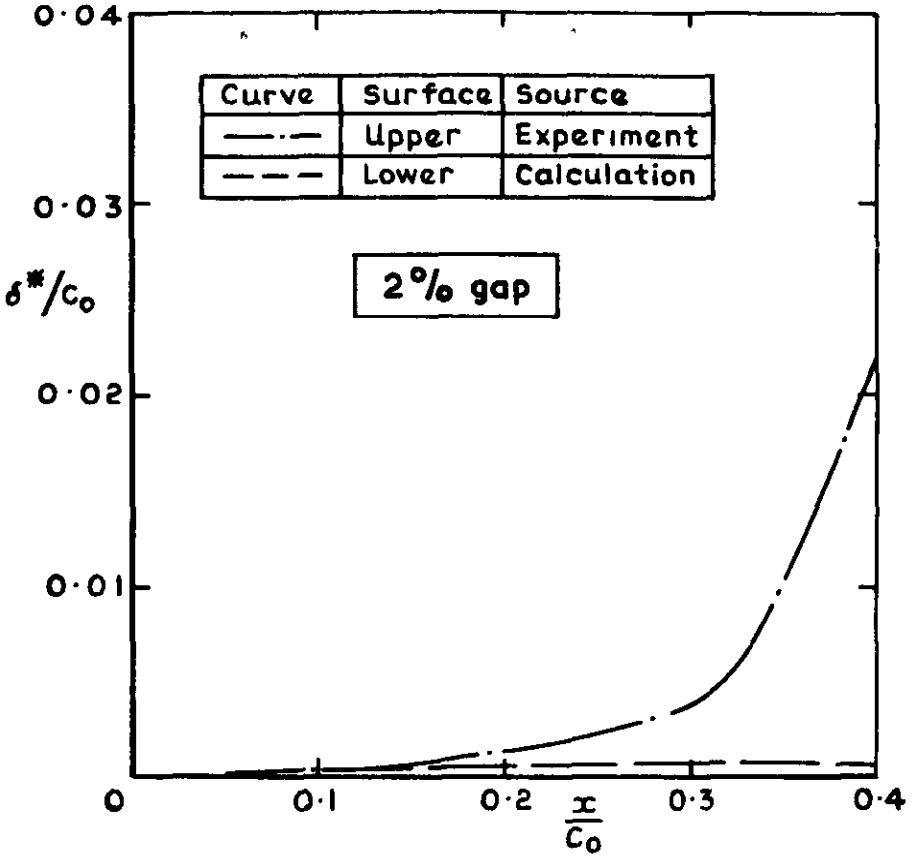

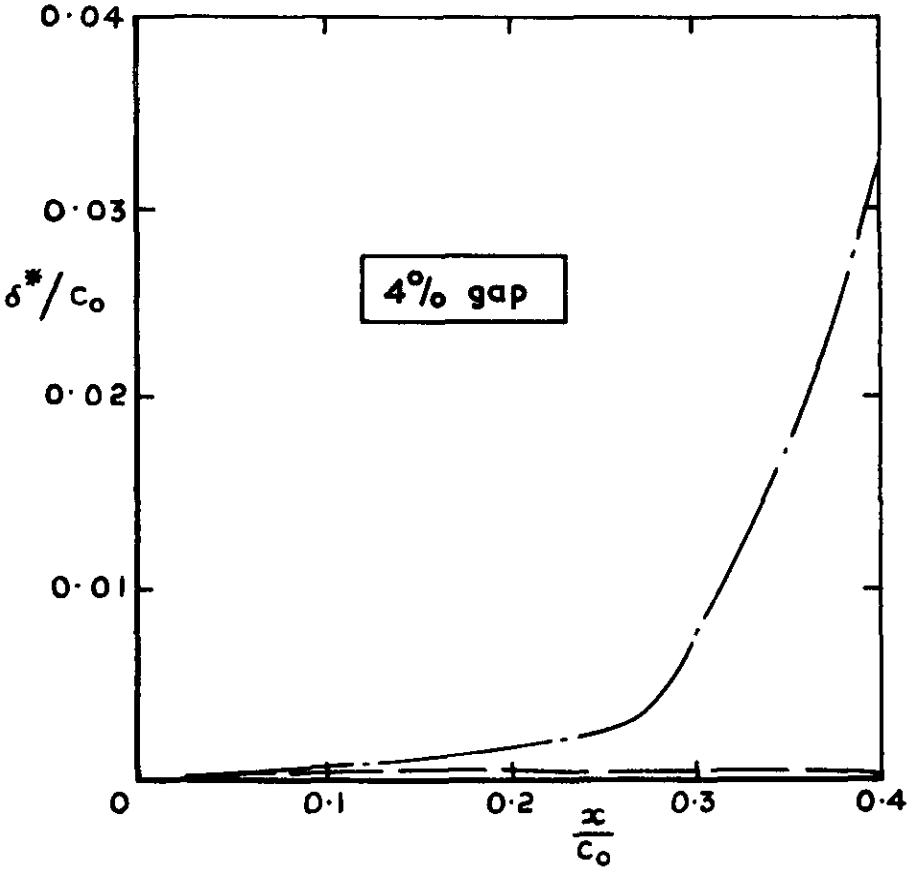

Fig. 11 Distributions of displacement thickness of flap boundary layer

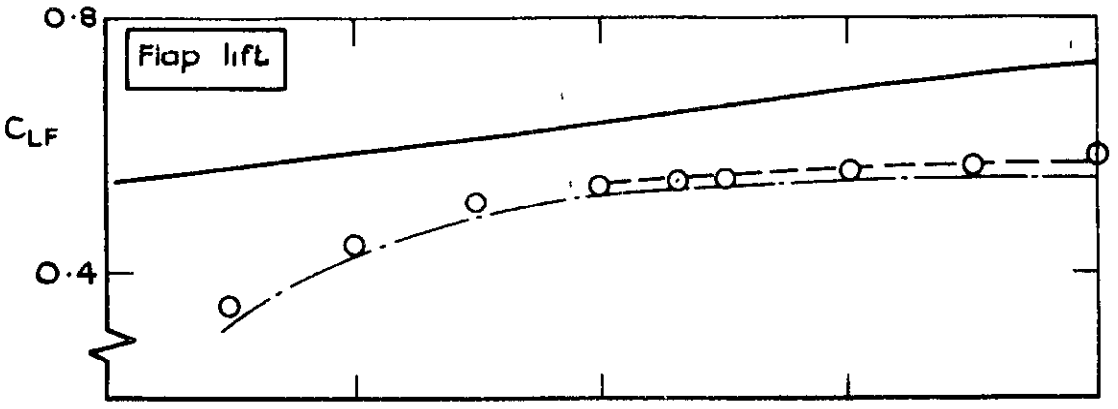

Curve or symbol	Derivation
———	(a). First inviscid approximation
— — —	(b). (a) Corrected for flap boundary layer
——·——	(c). (b) Corrected for aerofoil wake (thin wake, close to flap)
⊙	Experiment

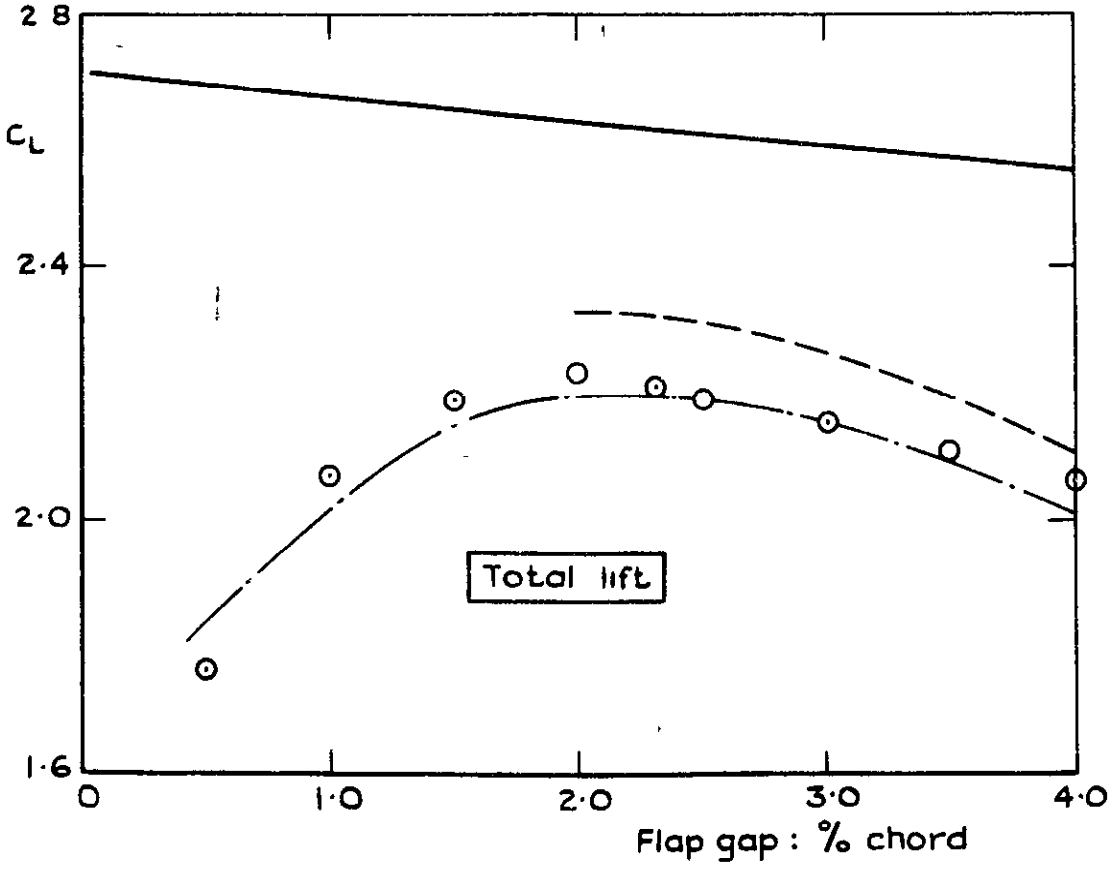

Fig. 12 Effect of flap boundary layer and aerofoil wake on lift

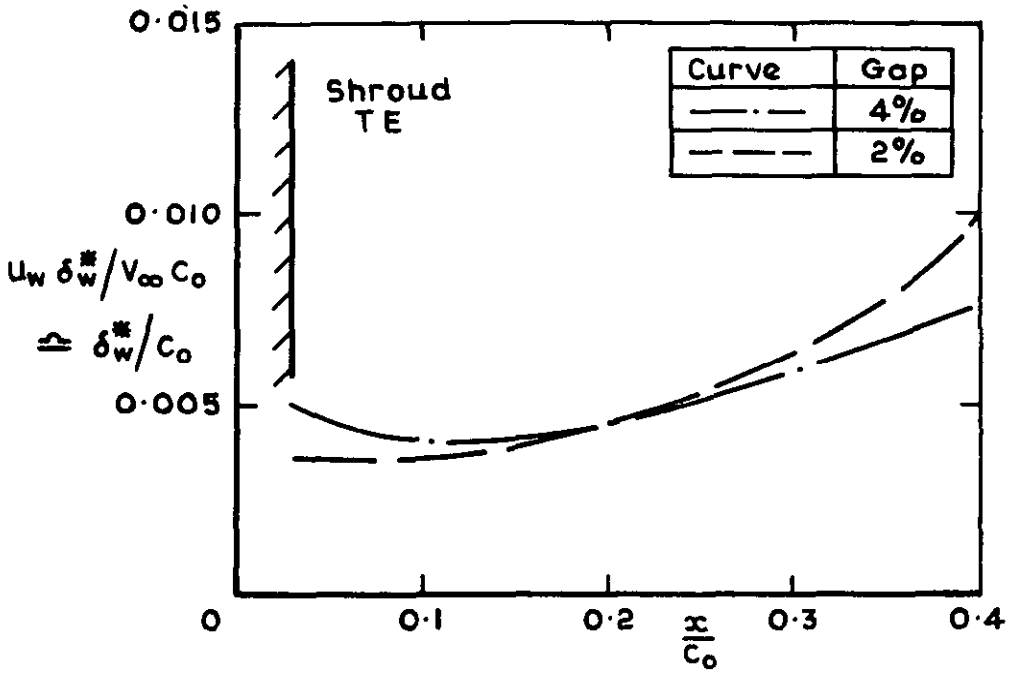

a Displacement thickness

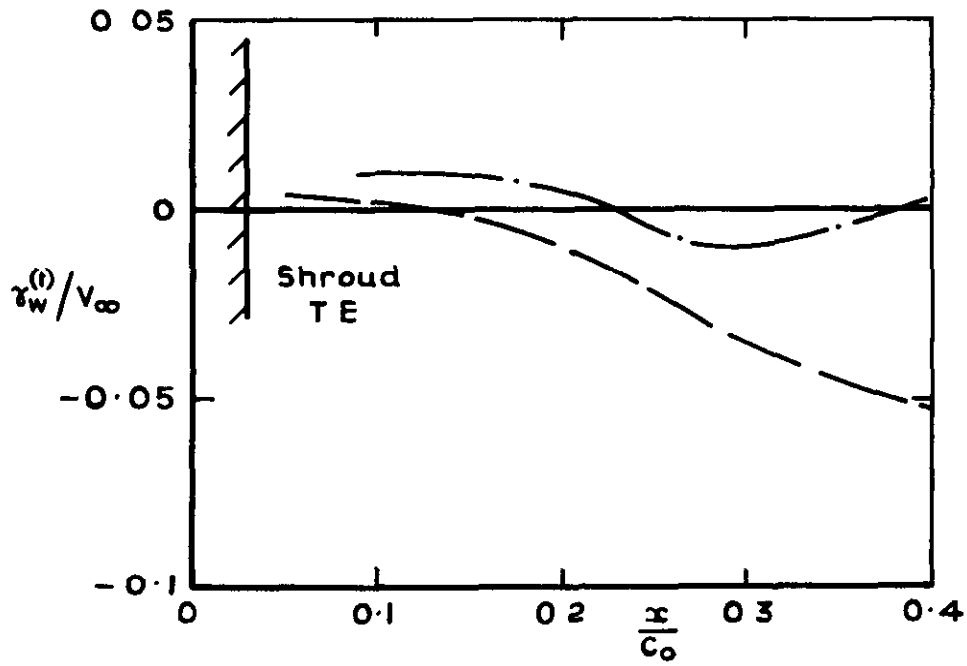

b Vortex strength of 'thin' wake

Fig.13a & b Experimentally - determined wake properties

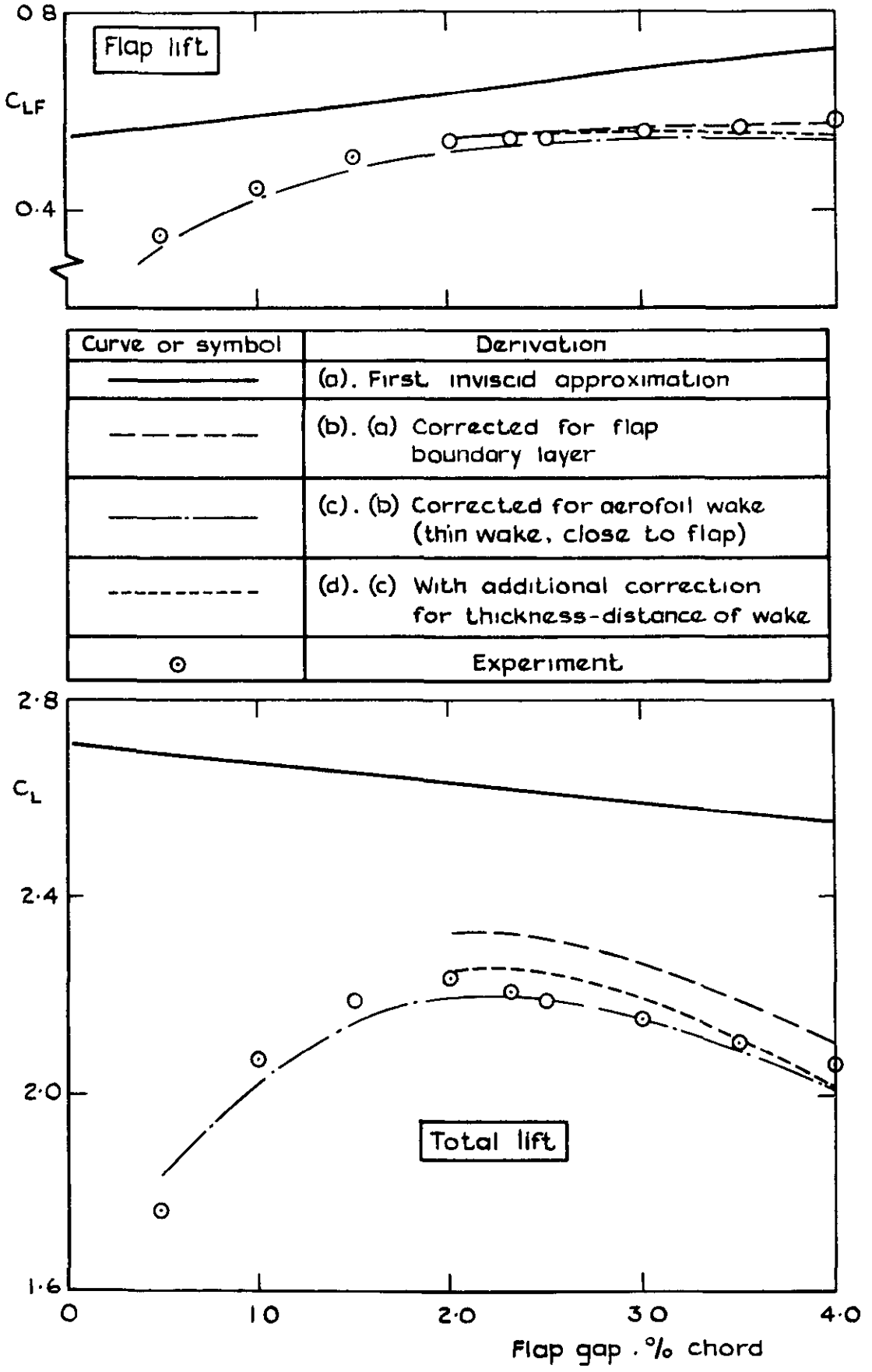

Fig. 14 Effect of flap boundary layer and aerofoil wake on lift

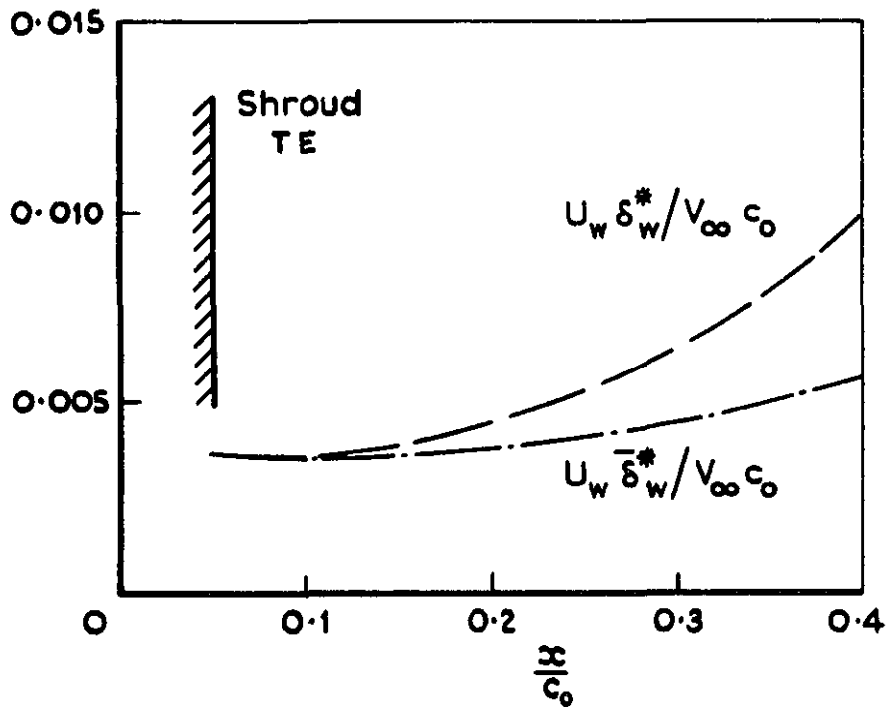

Fig.15 Influence of 'thickness - distance' correction on effective displacement thickness of aerofoil wake; 2% gap

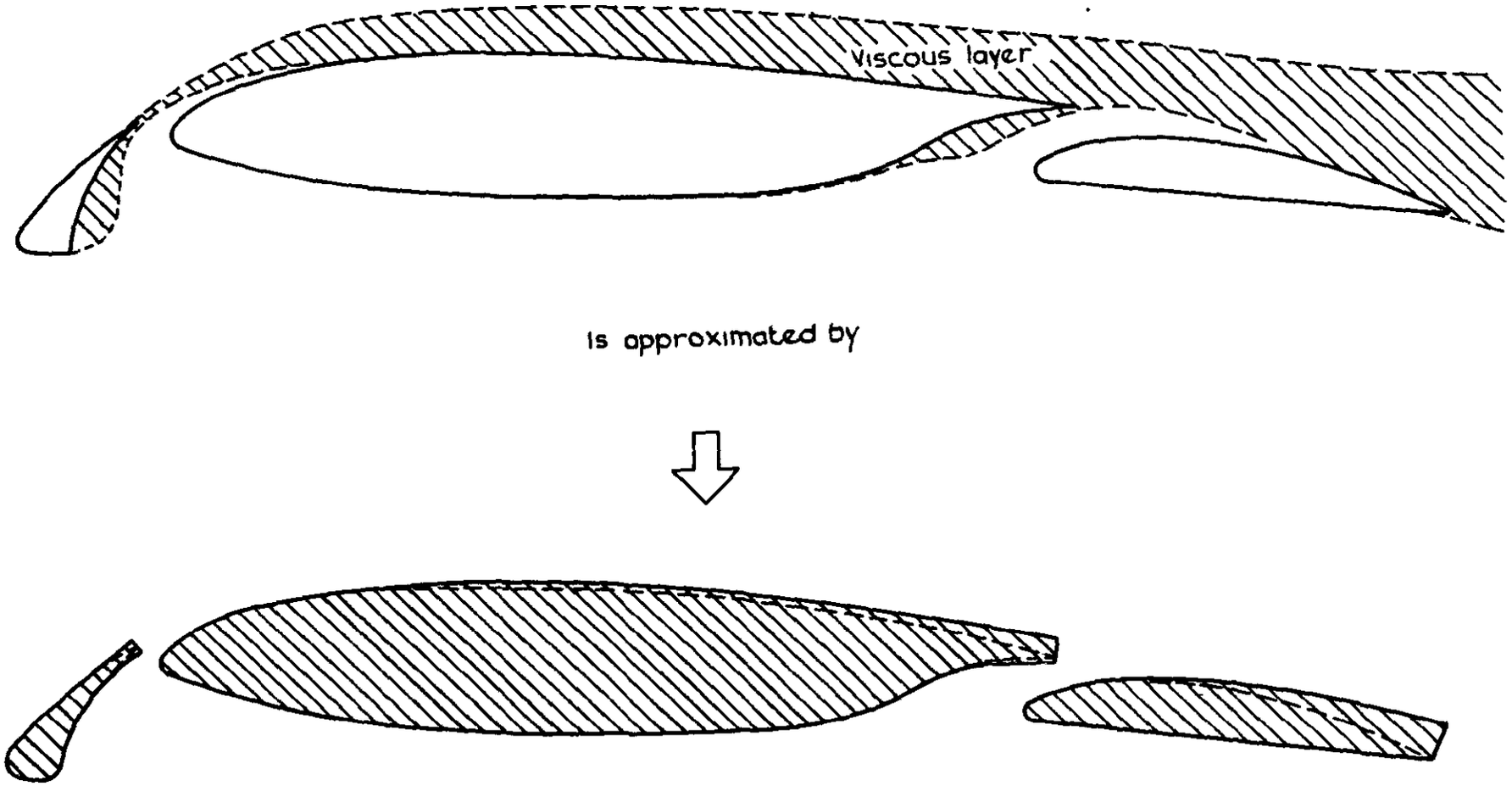

Fig. 16 Representation of viscous layer by a displacement profile

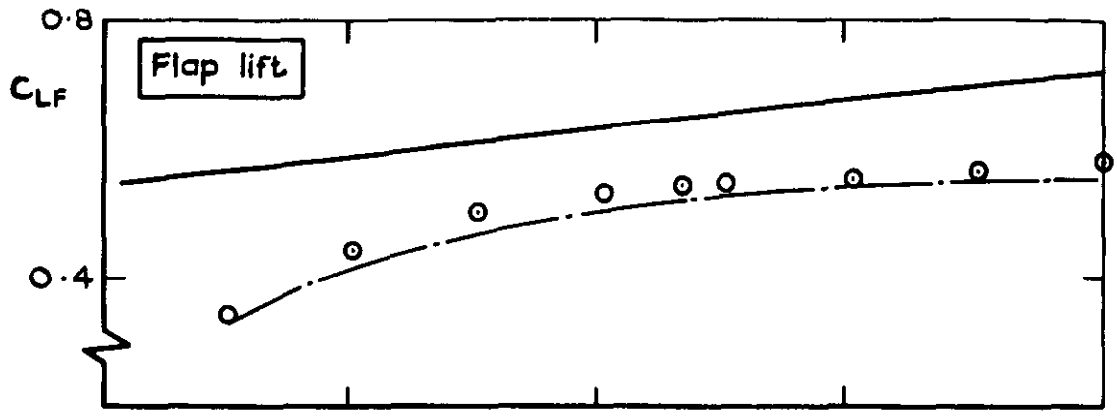

Symbol	Derivation
⊙	Experiment
———	First inviscid approximation
—·—	Displacement correction

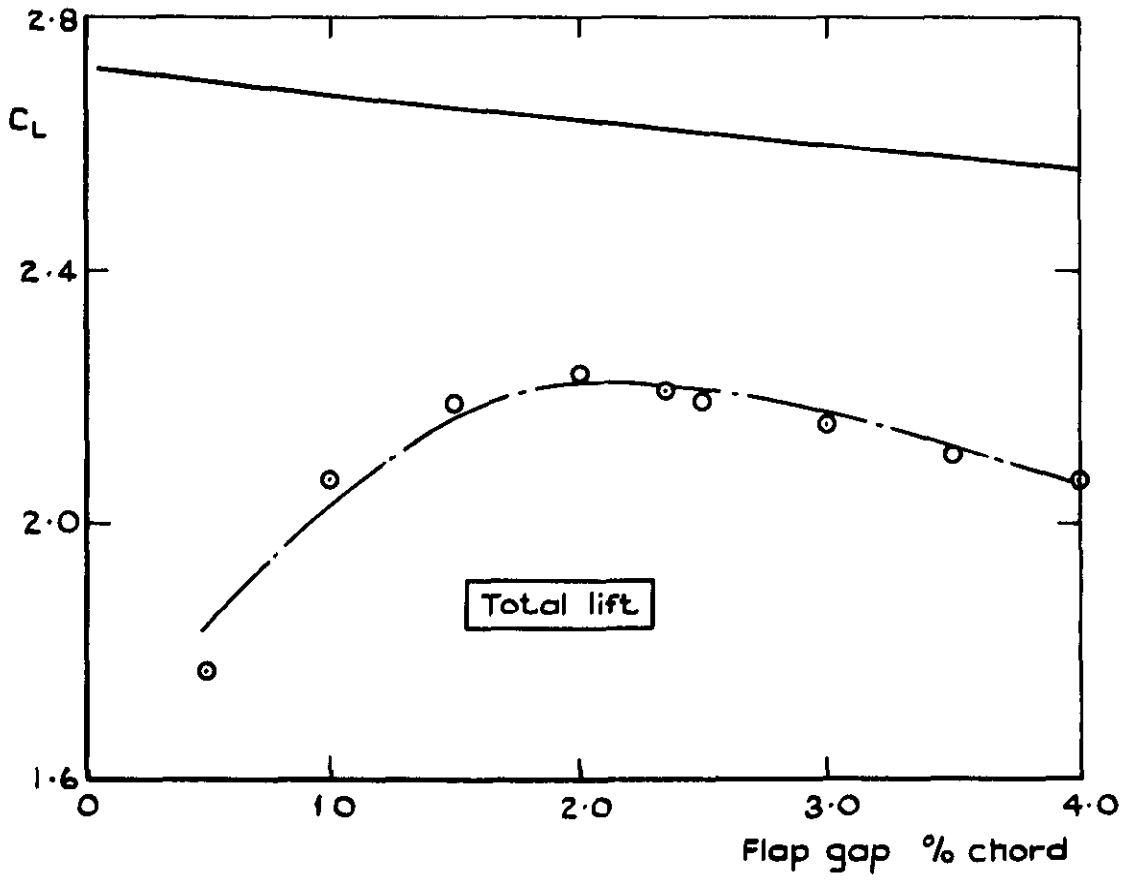

Fig. 17 Effect of flap boundary layer and aerofoil wake on lift

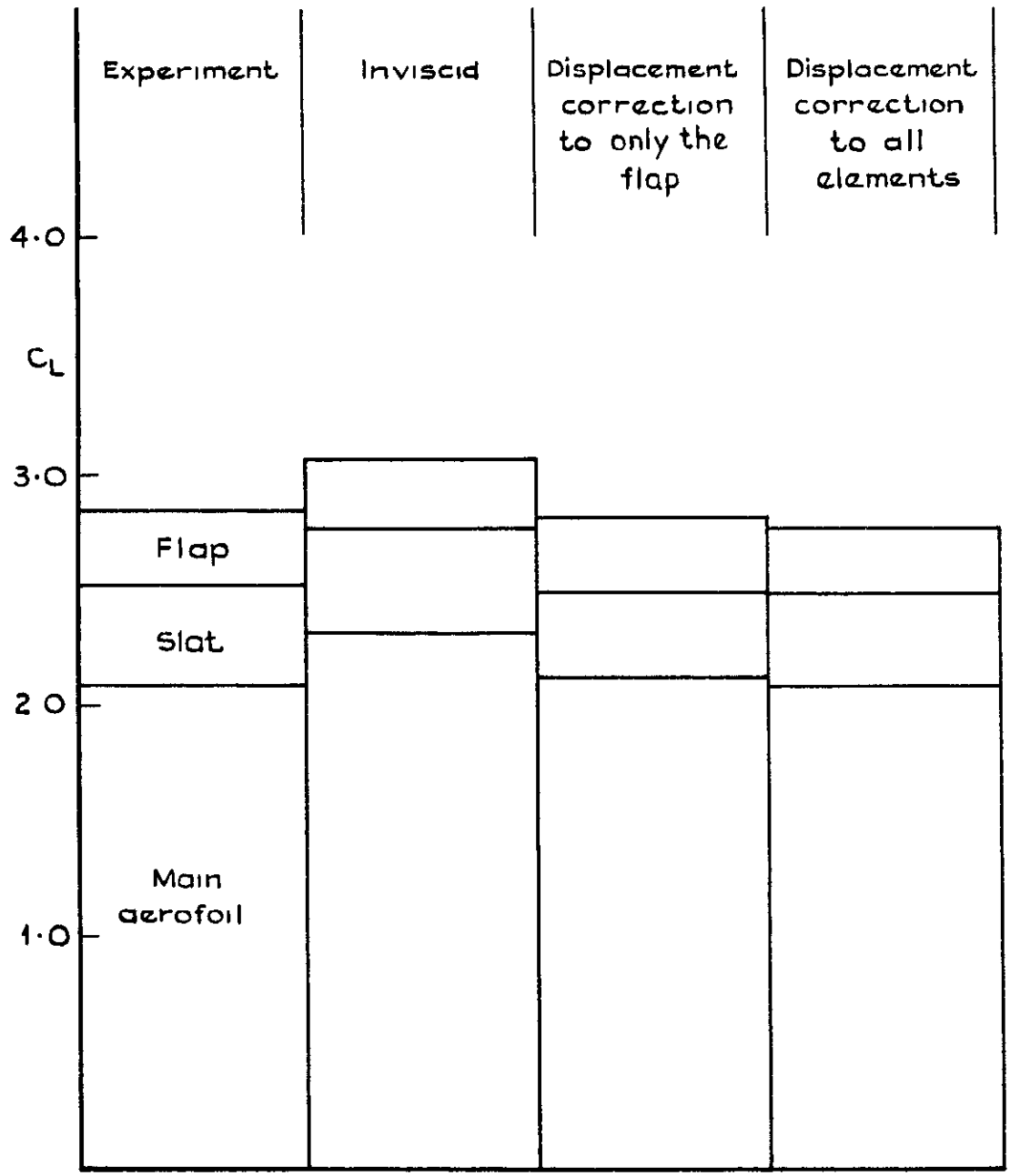

Fig.18 Effect of correction for boundary layers and wakes on C_L of an aerofoil with slat and flap

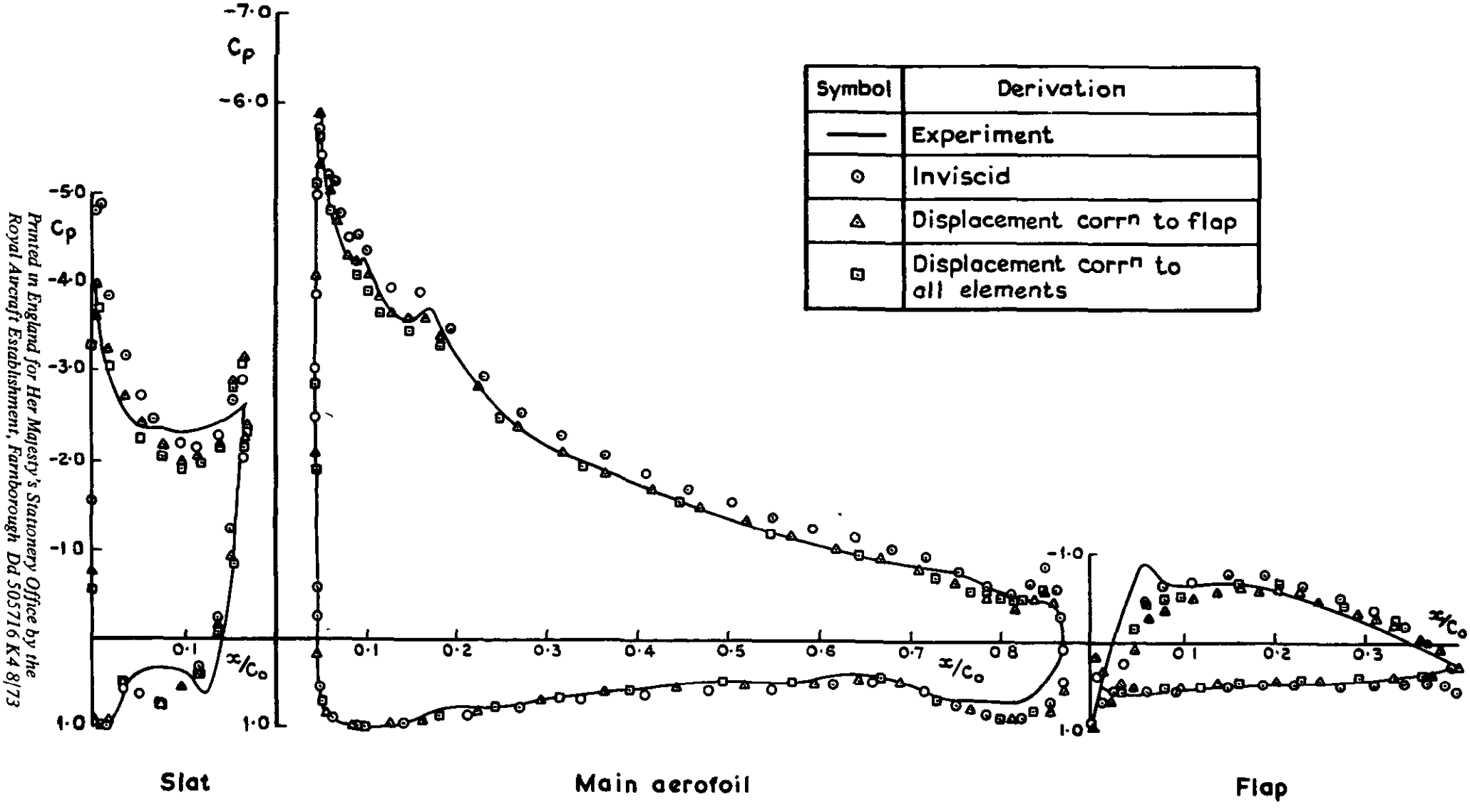

Printed in England for Her Majesty's Stationery Office by the Royal Aircraft Establishment, Farnborough Dd 505716 K4 8/73

Fig.19 Pressure distribution for slatted aerofoil with flap at 10° deflection

ARC CP No 1258
December 1972

533 695 16
532.526
532 5 032

Foster, D N
Ashill, P R
Williams, B R

THE NATURE, DEVELOPMENT AND EFFECT OF THE VISCOUS FLOW AROUND AN AEROFOIL WITH HIGH-LIFT DEVICES

This paper commences by describing the nature of the viscous flow around an aerofoil with high-lift devices, and considers a method of calculating the development of the viscous layers The contributions of the wing wake and flap boundary layer to the lift carried by the components of the multiple aerofoil are then examined, and finally the manner in which the viscous layers may be incorporated into a calculation of the loading on the aerofoil is discussed

Cut here

ARC CP No 1258
December 1972

533 695 16
532.526
532 5 032

Foster, D N.
Ashill, P R.
Williams, B. R

THE NATURE, DEVELOPMENT AND EFFECT OF THE VISCOUS FLOW AROUND AN AEROFOIL WITH HIGH-LIFT DEVICES

This paper commences by describing the nature of the viscous flow around an aerofoil with high-lift devices, and considers a method of calculating the development of the viscous layers The contributions of the wing wake and flap boundary layer to the lift carried by the components of the multiple aerofoil are then examined, and finally the manner in which the viscous layers may be incorporated into a calculation of the loading on the aerofoil is discussed

ARC CP No 1258
December 1972

533 695.16
532 526
532 5.032

Foster, D N
Ashill, P R.
Williams, B R

THE NATURE, DEVELOPMENT AND EFFECT OF THE VISCOUS FLOW AROUND AN AEROFOIL WITH HIGH-LIFT DEVICES

This paper commences by describing the nature of the viscous flow around an aerofoil with high-lift devices, and considers a method of calculating the development of the viscous layers The contributions of the wing wake and flap boundary layer to the lift carried by the components of the multiple aerofoil are then examined, and finally the manner in which the viscous layers may be incorporated into a calculation of the loading on the aerofoil is discussed

Cut here

DETACHABLE ABSTRACT CARDS

DETACHABLE ABSTRACT CARDS

1974

Published by
HER MAJESTY'S STATIONERY OFFICE

To be purchased from
49 High Holborn, London WC1V 6HB
13a Castle Street, Edinburgh EH2 3AR
41 The Hayes, Cardiff CF1 1JW
Brazennose Street, Manchester M60 8AS
Southey House, Wine Street, Bristol BS1 2BQ
258 Broad Street, Birmingham B1 2HE
80 Chichester Street, Belfast BT1 4JY
or through booksellers

C.P. No. 1258

SBN 11 470816 9